



Deposited via The University of York.

White Rose Research Online URL for this paper:

<https://eprints.whiterose.ac.uk/id/eprint/137799/>

Version: Accepted Version

Article:

Amesbury, M, Booth, R, Roland, T et al. (2018) Towards a Holarctic synthesis of peatland testate amoeba ecology: development of a new continental-scale palaeohydrological transfer function for North America and comparison to European data. *Quaternary Science Reviews*. pp. 483-500. ISSN: 0277-3791

<https://doi.org/10.1016/j.quascirev.2018.10.034>

Reuse

This article is distributed under the terms of the Creative Commons Attribution-NonCommercial-NoDerivs (CC BY-NC-ND) licence. This licence only allows you to download this work and share it with others as long as you credit the authors, but you can't change the article in any way or use it commercially. More information and the full terms of the licence here: <https://creativecommons.org/licenses/>

Takedown

If you consider content in White Rose Research Online to be in breach of UK law, please notify us by emailing eprints@whiterose.ac.uk including the URL of the record and the reason for the withdrawal request.

1 **Towards a Holarctic synthesis of peatland testate amoeba ecology:**
2 **development of a new continental-scale palaeohydrological transfer function**
3 **for North America and comparison to European data**

4
5 Matthew J. Amesbury ^{a,b*}, Robert K. Booth ^c, Thomas P. Roland ^a, Joan Bunbury ^{d,e}, Michael J.
6 Clifford ^f, Dan J. Charman ^a, Suzanne Elliot ^g, Sarah Finkelstein ^h, Michelle Garneau ⁱ, Paul D. M.
7 Hughes ^j, Alexandre Lamarre ^k, Julie Loisel ^l, Helen Mackay ^m, Gabriel Magnan ⁱ, Erin R. Markel
8 ^c, Edward A. D. Mitchell ^{n,o}, Richard J. Payne ^{p,q}, Nicolas Pelletier ^r, Helen Roe ^g, Maura E.
9 Sullivan ^c, Graeme T. Swindles ^s, Julie Talbot ^t, Simon van Bellen ⁱ, Barry G. Warner ^u

10
11 * Corresponding author: Email: m.j.amesbury@exeter.ac.uk (M. J. Amesbury).

12
13 ^a Geography, College of Life and Environmental Sciences, University of Exeter, UK

14 ^b Environmental Change Research Unit (ECRU), Faculty of Biological and Environmental Sciences,
15 University of Helsinki, Finland

16 ^c Earth and Environmental Sciences, Lehigh University, USA

17 ^d Department of Geography and Earth Science, University of Wisconsin – La Crosse, USA

18 ^e Department of Geography, University of Toronto, Canada

19 ^f Desert Research Institute, Nevada, USA

20 ^g School of Natural and Built Environment, Queen's University Belfast, UK

21 ^h Department of Earth Sciences, University of Toronto, Canada

22 ⁱ Geotop, Université du Québec à Montréal, Canada

23 ^j Geography and Environment, University of Southampton, UK

24 ^k Environment and Climate Change Canada, Canada

25 ^l Department of Geography, Texas A&M University, USA

26 ^m School of Geography, Politics and Sociology, University of Newcastle, UK

27 ⁿ Institute of Biology, Faculty of Science, University of Neuchâtel, Switzerland

28 ^o Botanical Garden of Neuchâtel, Switzerland

29 ^p Environment, University of York, UK

30 ^q Department of Biology, Penza State University, Russia

31 ^r Department of Geography and Environmental Studies, Carleton University, Canada

32 ^s School of Geography, University of Leeds, UK

33 ^t Department of Geography, Université de Montréal, Canada

34 ^u Earth and Environmental Sciences, University of Waterloo, Canada

35
36 **Author contributions:** MJA and RKB conceived the work and compiled/archived the data. MJA
37 conducted data analysis and wrote the manuscript. All authors contributed data, actively discussed the
38 direction of the research and/or contributed to manuscript editing.

39
40 **Keywords:** North America, testate amoebae, peatland, water table, transfer function, ecology,
41 biogeography, cosmopolitanism.

42
43 **Highlights**

- 44
45
46
47
48
- Dataset of ca. 2000 North American peatland testate amoeba surface samples compiled
 - Palaeohydrological transfer functions tested statistically, applied to independent palaeo data
 - New model an effective tool for palaeohydrological reconstruction across North America
 - Biogeographical patterns occur at taxonomic resolution applied; taxa hydrological optima mostly robust across North America

- Combined North American and European dataset illustrates potential for Holarctic synthesis

Abstract

Fossil testate amoeba assemblages have been used to reconstruct peatland palaeohydrology for more than two decades. While transfer function training sets are typically of local- to regional-scale in extent, combining those data to cover broad ecohydrological gradients, from the regional- to continental- and hemispheric-scales, is useful to assess if ecological optima of species vary geographically and therefore may have also varied over time. Continental-scale transfer functions can also maximise modern analogue quality without losing reconstructive skill, providing the opportunity to contextualise understanding of purely statistical outputs with greater insight into the biogeography of organisms. Here, we compiled, at moderate taxonomic resolution, a dataset of nearly 2000 modern surface peatland testate amoeba samples from 137 peatlands throughout North America. We developed transfer functions using four model types, tested them statistically and applied them to independent palaeoenvironmental data. By subdividing the dataset into eco-regions, we examined biogeographical patterns of hydrological optima and species distribution across North America. We combined our new dataset with data from Europe to create a combined transfer function. The performance of our North-American transfer function was equivalent to published models and reconstructions were comparable to those developed using regional training sets. The new model can therefore be used as an effective tool to reconstruct peatland palaeohydrology throughout the North American continent. Some eco-regions exhibited lower taxonomic diversity and some key indicator taxa had restricted ranges. However, these patterns occurred against a background of general cosmopolitanism, at the moderate taxonomic resolution used. Likely biogeographical patterns at higher taxonomic resolution therefore do not affect transfer function performance. Output from the combined North American and European model suggested that any geographical limit of scale beyond which further compilation of peatland testate amoeba data would not be valid has not yet been reached, therefore advocating the potential for a Holarctic synthesis of peatland testate amoeba data. Extending data synthesis to the tropics and the Southern Hemisphere would be more challenging due to higher regional endemism in those areas.

100 1. Introduction

101 Testate amoebae are a polyphyletic group of microscopic, unicellular protists that occur globally in a
102 range of soils, rivers, lakes and wetlands, including ombrotrophic peatlands – environments which are
103 frequently used to reconstruct Holocene palaeohydrological change (Mitchell et al., 2008). These
104 reconstructions are based on a transfer function approach, inherent in which is a robust understanding
105 of peatland testate amoeba ecology, particularly as it relates to target reconstruction variables,
106 principally water table depth (WTD).

107
108 Local- or regional-scale transfer function models around the globe have provided robust
109 palaeohydrological reconstructions based on the strong empirical relationship between independent
110 (i.e. WTD) and response (i.e. testate amoeba community change) variables (e.g. Swindles et al., 2009,
111 2014; van Bellen et al., 2014; Li et al., 2015). However, reconstruction magnitude can vary when local-
112 and regional-scale models are applied outside of their training set range (Turner et al., 2013), providing
113 a strong motivation to develop broader-scale, compiled models that provide standard reconstruction
114 tools with directly comparable results.

115
116 **Modern analogues from sites close to a core location may potentially better represent the**
117 **contemporary environment than those from more distant sites in the present day. However, as we go**
118 **back in time through different climate and ecological boundary conditions, as any transfer function**
119 **reconstruction inevitably aims to do, local modern analogues may be less appropriate and it becomes**
120 **more likely that better analogues will be found in different regions. Therefore, whilst local- and regional-**
121 **scale models perform well statistically in cross-validation, the same performance cannot be assumed**
122 **for downcore reconstructions and large-scale datasets/models should yield more reliable**
123 **reconstructions for any given location given their greater range of modern analogues. However, as the**
124 **geographical extent of training sets is increased to the continental-, hemispheric- or even global-scales,**
125 **it may become more problematic to effectively model independent and response variable relationships**
126 **due to the introduction of confounding factors such as latitude and temperature effects, secondary**
127 **environmental gradients or non-linear processes such as permafrost and fire. Therefore, there may be**
128 **a geographical range limit beyond which the compilation of modern testate amoeba and associated**
129 **environmental data is no longer beneficial for model development. Recently, it has been shown that the**
130 **development of continental-scale transfer functions may have advantages over the use of local- or**
131 **regional-scale models (Amesbury et al., 2016). In particular, large training sets (i.e. > 1000 samples)**
132 **capture a greater range of variability in target environmental variables and include more modern**
133 **analogues for taxa that may be abundant in fossil records but that can be rare or absent in modern**
134 **datasets (Charman et al., 2007; Swindles et al., 2015a), potentially improving palaeohydrological**
135 **reconstructions.**

136
137 In addition, although individual transfer functions statistically model the relationship between modern
138 testate amoeba assemblages and WTD, a broader contextual understanding of peatland testate amoeba
139 ecology and biogeography is important. For example, recent research has shown that certain taxa, or
140 groups of taxa, may react to environmental change at different timescales (Sullivan and Booth, 2011;
141 Marcisz et al., 2014) or have geographically restricted or skewed ranges (Booth and Zygmunt, 2005;
142 Amesbury et al., 2016; Beyens and Bobrov, 2016), even extending to regional endemism, particularly in
143 the tropics and Southern Hemisphere (Smith and Wilkinson, 2007; van Bellen et al., 2014; Reczuga et
144 al., 2015). However, these ecological and biogeographical intricacies are not explicit in strictly statistical
145 reconstructions. Indeed, research has shown that continental-scale geographical patterns of both
146 genotypic and phenotypic diversity exist within seemingly cosmopolitan taxa (Heger et al., 2013; Roland

147 et al., 2017; Singer et al., 2018). In the case of *Hyalosphenia papilio* (Heger et al., 2013), this is a finding
148 potentially supported by a regionally skewed distribution of the same taxon across Europe (Amesbury
149 et al., 2016).

150
151 Greater insight into wide-scale biogeographical patterns of soil protists is a fundamental research
152 domain (Geisen et al., 2017). An increasing number of studies have used protists (Foissner, 2006, 2008),
153 and specifically testate amoebae (e.g. Smith and Wilkinson, 2007; Fournier et al., 2015; Fernández et
154 al., 2016; Lara et al., 2016), to argue against the 'everything is everywhere: but the environment selects'
155 paradigm (Baas Becking, 1934; see also De Wit and Bouvier, 2006; O'Malley, 2007, 2008). Research
156 communities can move towards a broader understanding of these patterns by working collaboratively
157 to make use of the ever-increasing amount of data from individual studies that can be compiled and
158 used to both develop new, robust reconstruction tools (Amesbury et al., 2016), as well as begin to
159 provide insight into important biogeographical debates (Smith et al., 2008). In addition, an
160 understanding of wide-scale peatland testate amoeba ecology and biogeography is important in order
161 to provide robust regional- to continental-scale palaeoclimatic interpretation of 1) palaeo-data
162 compilations (e.g. Swindles et al., 2013), 2) studies from individual sites or groups of sites aiming to
163 study the Holocene evolution of regional-scale climate systems (e.g. Magnan and Garneau, 2014; van
164 Bellen et al., 2016), 3) studies investigating anthropogenic drainage (e.g. Laggoun-Défarge et al., 2008;
165 Payne et al., 2010; Talbot et al., 2010) and 4) studies of ecohydrological changes from specific climatic
166 disturbances such as permafrost thaw (Lamarre et al., 2012; Swindles et al., 2015b; Pelletier et al., 2017;
167 Zhang et al., 2018).

168
169 Building on the development of a recent pan-European transfer function (Amesbury et al., 2016), here
170 we apply a similar approach to the North American continent. Through a wide collaborative network,
171 we have compiled almost 2000 published and unpublished testate amoeba surface samples from 137
172 sites covering 34° of latitude and almost 100° of longitude. Our objectives are to (1) describe the ecology
173 of peatland testate amoebae in North America in terms of the key environmental variable, water table
174 depth; (2) develop a new, rigorously tested continental-scale transfer function for reconstructing
175 ombrotrophic peatland palaeohydrology; and (3) as the first step towards a Holarctic synthesis, assess
176 the ecology and biogeography of testate amoeba across two continents by combining our new North-
177 American dataset with data from a pan-European synthesis (Amesbury et al., 2016) to create a
178 combined dataset with >3700 samples in total.

179
180

181 **2. Methods**

182 183 **2.1. Data compilation and taxonomy**

184 We collated a total dataset of 1956 modern surface samples from 137 peatlands located throughout
185 the Canada and the USA (Figure 1; Table 1). Peatlands included were predominately *Sphagnum*-
186 dominated and ombrotrophic, but data from other site types was also included (e.g. Booth and
187 Zygmont, 2005). Data were compiled from 15 published sources in addition to four unpublished datasets
188 (Table 1). All original datasets, including previously unpublished datasets, in percentage data form and
189 a majority also as raw count data, have been archived and are freely available on the Neotoma
190 Paleocology Database (www.neotomadb.org). Raw count data was available for 1844 of 1956 samples
191 (excluding the datasets of Warner, 1987 and Payne et al., 2006). For those samples, the mean count
192 was 148 individuals. Only 65 samples had a count <100, with a minimum count in any one sample of 52
193 individuals. All testate amoeba surface samples had an associated water table depth (WTD) value, with
194 a smaller number (n = 1859) also having an associated pH value. **Although some datasets contained**

195 other potential environmental variables (e.g. electrical conductivity, vegetation type), these data were
196 not frequent enough across the entire dataset to permit inclusion in the data analysis.
197

198 [INSERT FIGURE 1]

199 **Figure 1:** Map showing the location of 137 sites included in the study (see Table 1 for full details). Sites
200 are colour-coded by United States Environmental Protection Agency (EPA) eco-region (see text for
201 details). Locations of two independent palaeo records at Lac Le Caron, Québec and Framboise, Nova
202 Scotia are also shown (black spots). For references to colour, readers are referred to the online version
203 of the article.
204

205 Since the multiple analysts involved in the original data collection (publication dates ranging over 30
206 years from 1987 – 2017) applied slightly varying taxonomic schemes, it was necessary to merge data
207 into a coherent taxonomy that was valid across all datasets. To do this, we followed the precedent set
208 by Amesbury et al. (2016) in a compilation of European peatland testate amoeba data, taking a low-
209 resolution approach and merging like taxa into groups wherever necessary. However, due to the
210 generally greater consistency between original taxonomies than was the case for Amesbury et al.
211 (2016), the relative extent of grouping required here was less, with a total of 72 taxa in the complete
212 merged dataset, of which 25 were groupings containing multiple taxa (Table 2). Despite the
213 improvement in taxonomic resolution from Amesbury et al. (2016), individual analysts should not count
214 samples to the taxonomic scheme used here, but rather define individual taxa to as great an extent as
215 possible (e.g. particularly within *Corythion* – *Trinema* type), grouping into this scheme for statistical
216 analysis only. Exceptions to the taxonomy of Amesbury et al. (2016), permitted by the relative
217 taxonomic consistency of the original datasets, were as follows:
218

- 219 1. *Arcella artocrea* was consistently identified in addition to *Arcella arenaria* type and *Arcella catinus*
220 type, so this division remained. However;
- 221 2. *Arcella catinus* type was identified in most datasets, whereas *Arcella arenaria* type was only
222 identified in two datasets, that did not include *Arcella catinus* type. Therefore, *Arcella arenaria* type
223 was merged into *Arcella catinus* type;
- 224 3. *Centropyxis cassis* type and *Centropyxis platystoma* type were consistently identified across all
225 datasets, so these divisions remained. *Centropyxis aerophila* type was only identified in two
226 datasets so was merged into *Centropyxis cassis* type;
- 227 4. *Cyclopyxis arcelloides* type was consistently split into *Cyclopyxis arcelloides* type, *Diffflugia*
228 *globulosa* type and *Phryganella acropodia* type so these divisions remained;
- 229 5. *Diffflugia pulex* type and *Hyalosphenia minuta* were consistently identified in addition to
230 *Cryptodiffflugia sacculus*, so all taxa remained and were not grouped into *Cryptodiffflugia sacculus*
231 type;
- 232 6. *Diffflugia pristis* type, *Pseudodiffflugia fulva* type and *Pseudodiffflugia fascicularis* type were
233 consistently identified in addition to *Diffflugia lucida* type, so all taxa remained and were not
234 grouped into *Diffflugia lucida* type;
- 235 7. *Diffflugia bacillifera* type and *Diffflugia rubescens* type were consistently identified in addition to
236 *Diffflugia oblonga* type, so all taxa remained and were not grouped into *Diffflugia oblonga* type;
- 237 8. *Euglypha strigosa* type and *Euglypha tuberculata* type were consistently identified in addition to
238 *Euglypha ciliata* type, *Euglypha compressa* and *Euglypha cristata*. *Euglypha strigosa* type and
239 *Euglypha tuberculata* type therefore remained as separate taxa, with *Euglypha ciliata* type
240 containing only *Euglypha ciliata* type, *Euglypha compressa* and *Euglypha cristata*;
- 241 9. *Nebela penardiana* type was consistently identified in addition to *Gibbocarina (Nebela) tubulosa*
242 type, so this division remained;

- 243 10. *Heleopera petricola* was consistently identified in addition to *Heleopera sphagni*, so this division
244 remained;
- 245 11. *Padaungiella (Nebela) waillesi* type was consistently identified in addition to *Padaungiella (Nebela)*
246 *lageniformis*, so this division remained;
- 247 12. *Planocarina (Nebela) marginata* type was consistently identified in addition to *Planocarina*
248 *(Nebela) carinata* type, so this division remained.

249
250 **Following a recent redefinition, we update the nomenclature of *Nebela militaris* to *Alabasta militaris***
251 **(Duckert et al., 2018 in press).** The complete dataset was screened for data quality and rare taxa. Eight
252 taxa were removed as they occurred in <1% of the total number of samples (i.e. <19 samples; Table S1).
253 Eleven samples were removed where taxonomic merging or deletion of taxa only identified to genera
254 (e.g. *Diffflugia* sp., *Euglypha* sp. etc.) resulted in a percentage total <90% (Table S2). A further 18 samples
255 with extreme WTDs below the 0.5th (-15 cm) or above the 99.5th (67 cm) percentiles of all WTD
256 measurements were removed to avoid undue influence of these samples in subsequent transfer
257 function development (Table S3). This data management resulted in a useable dataset of 64 taxa and
258 1927 samples (Figure 2). Hereafter, this will be referred to as the full dataset. Of these 1927 samples,
259 all, with the exception of those from Warner and Charman (1994), had a known site location. It was not
260 possible to assign samples to exact sites for the Warner and Charman (1994) data due to unspecific
261 sample codes. Therefore, in all analyses requiring geographical information, reduced datasets were
262 used that excluded those samples.

263
264 [INSERT FIGURE 2]

265 **Figure 2:** Percentage distribution of all samples (n = 1927) and taxa (n = 64), ordered vertically by water
266 table depth (wettest samples at the top) and horizontally by water table depth optima from a WA-Tol
267 (inv) model of the full dataset (wettest optima at the left; see also Figure 5).

268
269 To investigate testate amoeba ecological and biogeographical patterns across North America and
270 Europe (Amesbury et al., 2016), we compiled the two continental-scale training sets to form a combined
271 dataset. We used the original merged datasets before the removal of rare taxa (n = 1799 for Europe, n
272 = 1956 for North America, total n = 3755), since combining the two may have resulted in additional
273 samples to characterise previously rare taxa. Given the greater degree of taxonomic grouping in the
274 European data, it was necessary to harmonise the North American data into the European taxonomic
275 scheme (Amesbury et al., 2016). Taxonomic changes made to facilitate this followed the reverse of the
276 12 numbered points above. In addition, three taxa not identified in Europe (*Coniococassis*
277 *pontigulasiformis*, *Nebela barbata* and *Waileseila eboracensis*) were added to the European taxonomy,
278 resulting in an initial 63 defined taxa/taxonomic groups. Once combined, we applied the same data
279 quality and rare taxa criteria as above and in Amesbury et al. (2016). We removed 11 rare taxa present
280 in <1% of the total number of samples (<37 samples), 35 samples with extreme WTDs below the 0.5th (-
281 15 cm) or above the 99.5th (82 cm) percentiles of all WTD measurements and a further 45 samples with
282 percentage totals <90% (see Tables S4 – S6 for details of removed samples/taxa). This resulted in a
283 workable combined dataset of 52 taxa and 3675 samples.

284
285 All biogeographical inferences resulting from this work should be set against the taxonomic resolution
286 applied. Light microscopic studies necessitate a practical, but relatively low-resolution approach when
287 set against known levels of cryptic and pseudo-cryptic diversity in testate amoebae (e.g. Heger et al.,
288 2013; Oliverio et al., 2014; Kosakyan et al., 2016; Singer et al., 2018). Therefore, where biogeographic
289 patterns are identified at the resolution applied, we can assume that these would still be valid at a higher
290 taxonomic resolution. However, if biogeographic patterns are absent for particular taxa, this does not
291 exclude possible evidence when true genetic diversity is examined.

292
293 **2.2. Statistical analyses**
294 Considering the key aim of this study to produce a transfer function for palaeohydrological
295 reconstruction, non-metric multidimensional scaling (NMDS) was used *sensu* Amesbury et al. (2016) to
296 objectively examine the dataset and potentially exclude outlying sites and/or samples that were non-
297 typical for the ombrotrophic peatlands commonly used in palaeoclimate research. NMDS was carried
298 out using the 'metaMDS' function in the R package *vegan* (Oksanen et al., 2015), with water table depth
299 and pH included as potential environmental drivers. Default settings and automatic data transformation
300 were applied and the analysis was conducted based on Bray-Curtis dissimilarity. Environmental variables
301 were passively fitted to the NMDS, and their significance tested, using the 'envfit' function in *vegan*.
302 Sample-specific values for the Shannon-Wiener diversity index (SWDI) were calculated using the
303 'diversity' function in *vegan*. Transfer function development was carried out using the R package *rioja*
304 (Juggins, 2015). Four common model types were applied; weighted averaging with and without
305 tolerance downweighting (WA/WA-Tol; both with potential for inverse (inv) or classical (cla)
306 deshrinking), weighted averaging with partial least squares (WAPLS), maximum likelihood (ML) and the
307 modern analogue technique (MAT; with the potential for a weighted-mean version, WMAT). For each
308 model, only the best performing version (judged by r^2 and leave-one-out root mean square error of
309 prediction; RMSEP_{LOO}) was selected for further analysis. Additional statistical testing followed
310 convention in the recent literature after Amesbury et al. (2013) and included calculation of leave-one-
311 site-out RMSEP (Payne et al., 2012; RMSEP_{LOSO}), segment-wise RMSEP (Telford and Birks, 2011;
312 RMSEP_{SW}) and a spatial autocorrelation test (Telford and Birks, 2005, 2009) using the 'rne' (random,
313 neighbour, environment) function in the R package *palaeoSig* (Telford, 2015). Also, following
314 convention, transfer function development followed a two-step process. We firstly developed models
315 using the full dataset and then, for each model type, performed a second, 'pruned', model run which
316 excluded samples with high residual values greater than 20% of the total range of measured water table
317 depths.

318
319 As part of the testing process, models were applied to independent (i.e. no modern samples from the
320 sites were included in the transfer function) palaeo-data from two *Sphagnum*-dominated ombrotrophic
321 peatlands: Framboise bog, Nova Scotia (45.7208°N, 60.5521°W; H. Mackay, unpublished) and Lac Le
322 Caron peatland, Québec (52.2884°N, 75.8393°W; van Bellen et al., 2011). Original taxonomies of the
323 independent palaeo datasets were merged and updated (i.e. in terms of nomenclature) as necessary in
324 order to match the taxonomic scheme of the new models produced here. Sample-specific errors for all
325 transfer function reconstructions were based on 1000 bootstrapping cycles. We compared our
326 reconstructions with output from the most geographically extensive published transfer function in
327 North America (Booth, 2008) and tested the significance of all new reconstructions (Telford and Birks,
328 2011b) using the 'randomTF' function in the R package *palaeoSig* (Telford, 2015; Payne et al., 2016).

329
330 To test for regional variability within the continental dataset, we developed regional models based on
331 United States Environmental Protection Agency (EPA) Level 1 eco-region sub-divisions
332 (www.epa.gov/eco-research/ecoregions), using the pruned WA-Tol (inv) model (excluding samples
333 from Warner and Charman, 1994; see Section 2.1) as the basis for regional model development ($n =$
334 1696). Our data covered eight different eco-regions but to ensure regional models were representative,
335 we only developed models for those regions containing >50 samples (Table 3). This resulted in five
336 regional models: taiga (samples $n = 68$, sites $n = 7$), northern forests (samples $n = 978$, sites $n = 56$),
337 northwestern forested mountains (samples $n = 136$, sites $n = 16$), marine west coast forest (samples $n =$
338 266, sites $n = 23$) and eastern temperate forests (samples $n = 377$, sites $n = 18$). Models were not
339 developed for the tundra (samples $n = 7$, sites $n = 1$), Hudson Plain (samples $n = 32$, sites $n = 7$) and
340 North American deserts (samples $n = 11$, sites $n = 1$) eco-regions. The independent palaeo records were

341 located in the northern forest (Framboise) and taiga (Lac Le Caron) eco-regions. The programme PAST
342 (v3.20; Hammer et al., 2001) was used to run one-way PERMANOVA tests (9999 iterations, assessed by
343 Bray-Curtis dissimilarity) of the differences between samples from different eco-regions.

344
345 To test the validity of a combined North American and European transfer function, we applied the North
346 American (this study), European (Amesbury et al., 2016) and a pruned combined model (n = 3425; all
347 WA-Tol (inv)) to independent palaeo data from both North America (Framboise) and Europe (Tor Royal
348 Bog, UK *sensu*. Amesbury et al., 2016). We also qualitatively compared the modelled taxa water table
349 depth optima and relative optima ranking of the three models.

350

351

352 **3. Results**

353

354 **3.1. Ordination**

355 Summary NMDS results are shown in Figure 3. For the NMDS of the full dataset (Figures 3A and 3B),
356 square root transformation was automatically applied. WTD was significantly correlated to NMDS axis
357 1 ($p < 0.001$), although the WTD vector was at 45 degrees to the horizontal, with taxa favouring drier
358 conditions in the top left of the ordination space and taxa favouring wetter conditions in the bottom
359 right (Figure 3B). In general, all samples fell in a large, fairly coherent single swarm of data, with no
360 significant outliers, or groups of outliers, though samples tended to cluster more in the uppermost part
361 of the swarm (Figure 3A). When sub-divided by eco-region (Figure 3C), there was a high degree of
362 overlap, with no regions outlying all others. Only samples from the northwestern forested mountain
363 eco-region tended to cluster in a specific part of the sample swarm (towards the left; Figure 3C), whereas
364 samples from all other regions were located throughout the ordination space. This high degree of
365 overlap, coupled with the significant correlation of WTD to NMDS axis 1 provided a strong justification
366 to continue with transfer function development using the full dataset.

367

368 [INSERT FIGURE 3]

369 **Figure 3:** NMDS biplots for A) the full dataset (n = 1927) showing sample positions, B) the full dataset
370 showing taxa positions, C) a reduced dataset excluding samples from Warner and Charman (1994) (n =
371 1884) showing sample positions, colour-coded by EPA eco-region (see text for details). Vectors on all
372 plots show correlation with environmental drivers. Some taxa positions in B have been marginally
373 altered to improve legibility, but relative positions remain intact. Full names for taxa abbreviations can
374 be found in Table 2. For references to colour, readers are referred to the online version of the article.

375

376 **3.2. Transfer function development**

377 Performance statistics for the best-performing version of each model type are shown in Table 4. For the
378 full dataset, the range of WTD values was 82 cm (minimum WTD -15cm; maximum WTD 67 cm),
379 therefore a value of 16.4 cm (20% of range) was used to remove outlier samples during data pruning.
380 The number of pruned samples varied for each individual model type (Table 4). Following data pruning,
381 the WMAT K5 (weighted-mean modern analogue technique with five nearest neighbours) model was
382 the best performing when judged by $RMSEP_{LOO}$ and R^2 . ML was the worst performing model (based on
383 $RMSEP_{LOO}$) when all samples were included but improved after data pruning (e.g. second best pruned
384 model for r^2 only), largely down to the removal of 410 samples with high residual values, more than
385 double the number of pruned samples than for the next highest model (WA-Tol (inv); n = 197). Pruned
386 samples for all models tended to be reasonably evenly distributed between wet and dry extremes,
387 however ML produced far more extreme negative residuals (i.e. samples where WTD was substantially
388 overestimated; Figure 4). Partly as a result, both ML and WMAT K5 suffered from comparatively high
389 average bias values when compared to the two WA-based models, although the WA-based models had

390 higher maximum bias (Table 4). WAPLS C2 and WA-Tol (inv) performed very similarly on all metrics, with
391 WA-Tol (inv) marginally outperforming WAPLS C2 after data pruning.

392
393 All models showed a decrease in relative performance for $RMSEP_{LOSO}$ and $RMSEP_{SW}$ compared to
394 $RMSEP_{LOO}$, though for ML, both reductions were marginal (Table 4). Relative performance ratings also
395 changed when different versions of RMSEP were applied. For example, when using $RMSEP_{LOSO}$, WA-
396 based models were the best performing, but using $RMSEP_{SW}$, both showed a higher relative decrease in
397 performance than WMAT K5 and ML (though $RMSEP_{SW}$ for the WA-based models was still lower than
398 for ML; Figure S1). Both WA-based models performed worse in 'dry' segments (i.e. WTDs greater than
399 40 cm) with comparatively less samples, whereas WMAT K5 and ML displayed more consistent RMSEP
400 values across all segments, suggesting that these models were not as affected by WTD and/or segment
401 sampling frequency (Figure S1). WMAT K5 performed relatively poorly for $RMSEP_{LOSO}$, suggesting that
402 this model type does not deal well with clustered training sets (Amesbury et al., 2016).

403
404 All models displayed evidence of spatial autocorrelation, given that r^2 declined much more rapidly when
405 geographically close compared to random samples were removed; this decline was sharpest for WMAT
406 K5 (Figure S2). R^2 values for WMAT K5 and ML declined steadily with the continued removal of
407 geographically close samples, whereas, interestingly, r^2 increased from previous values for both WA-
408 based models when all samples within 1000 km of each other were removed, such that the 1000 km
409 values were higher than for 100 km. Even values at 2500 km (i.e. the models would only contain samples
410 that are >2500 km apart) were comparable to 100 km. These results suggest that, despite the initial
411 decline in r^2 , the WA-based models are more robust to spatial autocorrelation than WMAT K5 or ML.

412
413 Taxon-specific values for WTD optima and tolerance showed taxa ordered along a WTD gradient both
414 comparable to the diagonal WTD vector along axis 1 of the NMDS (Figure 3) and also to other studies.
415 In contrast to a European compilation (Amesbury et al., 2016), where taxonomic grouping resulted in
416 more similar tolerance ranges along the WTD gradient, tolerances in this dataset (Figure 5) showed a
417 more typical pattern of being wider for drier taxa and vice versa (Mariusz Lamentowicz and Mitchell,
418 2005). For example, the mean tolerance for the driest half of taxa, ranked by optima, was 12.5 cm,
419 whereas the same value for the wettest half was 8.4 cm (significantly different at $p < 0.05$ for a two-
420 sample, two-tailed t-test, $df = 60$).

421
422 [INSERT FIGURES 4 AND 5]

423 **Figure 4:** Biplots of leave-one-out cross-validated observed versus predicted water table depth (left)
424 and residual error plots (right) for the four model types under investigation. See text for model
425 abbreviations. Orange points are model runs with all data, black points are model runs after the removal
426 of samples with high residual values. For references to colour, readers are referred to the online version
427 of the article.

428
429 **Figure 5:** Water table depth optima and tolerances (cm) for 64 taxa based on the WA-Tol (inv) model
430 after the removal of outlying samples ($n = 1730$).

431 432 3.3. Testing model application

433 All four models were applied to independent palaeo records from Framboise and Lac Le Caron peatlands
434 (Figure 1) and compared to reconstructions using the transfer function of Booth (2008), the most
435 geographically extensive published transfer function from North America (Figure 6; Figure S3). All model
436 types, as well as the Booth (2008) reconstructions, showed broadly similar patterns of change (Figures
437 6 and S3). WMAT K5 and ML reconstructions tended to reconstruct somewhat more abrupt (i.e. change
438 over less samples) and extreme (i.e. higher and lower water table depth values at either end of the

439 scale) change, when compared to the WA-based models, a trend particularly evident in the Lac Le Caron
440 reconstructions. In general, all four model types tended to co-vary within a range of 5 – 10 cm, however
441 there were periods when particular reconstructions were more divergent. For example, at 10 cm depth
442 at Framboise, the WMAT K5 model reconstructed a significant dry shift not seen in other models (Figure
443 6A) and at Lac Le Caron, the ML model produced wet shifts at 36 cm and around 215 cm that were not
444 replicated by other models, as well as reconstructing generally wetter conditions for the lower ~150 cm
445 of the profile (Figure 6B). However, when viewed as z-scores (Figure 6C and D; Swindles et al., 2015a),
446 the majority of shifts were aligned, suggesting that all models are reliably reconstructing the main
447 patterns of palaeohydrological change in the profiles.

448
449 [INSERT FIGURE 6]
450 **Figure 6:** Comparison of transfer function reconstructions from four model types. A and B are raw water
451 table values (cm). C and D are z-scores. A and B include comparison to reconstruction from Booth (2008).
452 A and C for Framboise bog, B and D for Lac Le Caron peatland. For all plots, higher y-axis water table
453 depth or z-score values indicate drier conditions. Note varying y-axis scales.

454
455 The significance of all reconstructions was tested against models trained on random data (Telford and
456 Birks, 2011b; Table 5). Reconstructions at Framboise for all model types were either significant (i.e.
457 <0.05) or very close to significant (0.057 for ML). However, equivalent *p* values at Lac Le Caron were
458 consistently insignificant, often to extremes. For example, ML had the lowest *p* value at 0.287 (despite
459 having the highest value at Framboise), with both WA-based models having *p* values > 0.98, meaning
460 their reconstructive ability was worse than almost all models trained on randomly generated data (see
461 also Payne et al., 2016).

462 463 3.4. Eco-region variability and models

464 One-way PERMANOVA tests showed that there were significant differences in testate amoeba
465 assemblages between factor eco-regions ($p < 0.0001$, $F = 15.16$). Species richness (i.e. number of taxa
466 present) differed among eco-regions whereas eco-region mean species diversity values were typically
467 more consistent (in the range 1.9 – 2, overall range for all samples 0.19 – 3.07), with the exception of
468 the northwestern forested mountains and North American deserts regions (Table 3). Those eco-regions
469 characterised by only a single site (tundra, North American deserts) had expectedly lower species
470 richness, but, in the case of the tundra region, still displayed species diversity equivalent to the total
471 dataset and to other regions (e.g. Swindles et al., 2009, 2014), despite being based on only seven
472 samples. There were notable differences in species richness among regions with more comparable
473 numbers of sites and samples. For example, eastern temperate forests (18 sites, 346 samples) contained
474 62 different taxa, whereas northwestern forested mountains (16 sites, 131 samples) contained only 42
475 taxa. In this case, the 20 fewer taxa in the northwestern forested mountains were often relatively rare
476 taxa that were absent from multiple regions, however also included the absence of other relatively
477 abundant taxa present in all other regions (e.g. *Amphitrema wrightianum*, *Bullinularia indica*, *Diffflugia*
478 *oblonga*, *Diffflugia pulex*). Inter-regional assemblage differences were investigated by plotting taxa
479 distributions across the eight eco-regions (Figure S5). Only eight of 64 taxa occurred in all eight eco-
480 regions: *Assulina muscorum*, *Nebela tinctoria* type, *Euglypha tuberculata*, *Hyalosphenia papilio*, *Corythion-*
481 *Trinema* type, *Centropyxis cassis* type, *Euglypha rotunda* type and *Diffflugia globulosa* type. However,
482 allowing for the reduced species richness in the less-sampled tundra and North American desert eco-
483 regions (Table 3; regions 1 and 8 on Figure S5), 42 of 64 taxa occurred in six or more eco-regions. Of the
484 22 taxa that were present in five or less eco-regions, 14 were absent from the less-sampled tundra and
485 North American desert regions, as well as the relatively taxa-poor northwestern forested mountains
486 region. Of those 14 taxa, the most frequent were *Physochila griseola* (619 (out of 1884) occurrences),
487 *Bullinularia indica* (519 occurrences) and *Centropyxis ecornis* type (376 occurrences). Taxa present in

488 only two or three eco-regions were largely driven by low occurrence, with only *Nebela minor* of that
489 group occurring in >100 samples (Figure S5).

490
491 Taxa tended to occur on a continuum where their presence in samples and eco-regions, and local
492 abundance, were broadly aligned (Figure S6). For example, common, locally abundant key hydrological
493 indicator taxa such as *Assulina muscorum*, *Trigonopyxis arcula* type and *Archerella flavum* tended to
494 occur in multiple (i.e. 6-8) eco-regions, whereas rare (in both occurrence and abundance) taxa such as
495 *Pseudodiffugia fascicularis* type and *Padaungiella lageniformis* type tended to have more restricted
496 ranges, occurring in only a few (i.e. 2-3) eco-regions. However, this overall trend also encompassed
497 considerable variability. Relatively rare taxa could still be locally abundant and occur across multiple
498 eco-regions. For example, *Arcella hemispherica* occurred in only 3% of samples, but had a maximum
499 abundance of 63% and was present in six eco-regions. Taxa that were rare in both occurrence and
500 abundance could still occur across multiple eco-regions. For example, *Quadrullella symmetrica* was
501 present in only 3.6% of samples, never above 9% abundance, but was only absent from one eco-region
502 (North American desert). The absence of *Q. symmetrica* from the North American desert eco-region is
503 noteworthy given the recent discovery of a *Quadrullella* taxon in a Mexican desert (Pérez-Juárez et al.,
504 2017). Finally, locally abundant taxa could also have more restricted ranges. For example, *Diffugia*
505 *oviformis* type occurred in only two eco-regions (NF and ETF), but formed more than half of the
506 assemblage in some samples in those regions.

507
508 To further test overall model performance and to further investigate internal biogeographical variability,
509 we developed models for five eco-regions, using only the WA-Tol (inv) model type (cf. Amesbury et al.,
510 2016; see Section 2.2). Eco-region model reconstructions varied notably (Figures 7 and S4), in terms of
511 value, pattern and, less often, direction of change. Most notably, the northwestern forested mountains
512 (NFM) model produced reconstructions, for both palaeo datasets, that had notably drier reconstructed
513 water table depth values when compared to all other models (including the pruned WA-Tol (inv) model
514 based on the full dataset; Figure 7A and B). Mean WTD for individual samples and the overall range of
515 WTDs sampled for the NFM model were equivalent to other models (Table 3), suggesting these
516 differences were not simply driven by poor characterisation of 'wet' conditions in the model. Even when
517 viewed as z-scores, the NFM model appeared anomalous, with often conflicting patterns and direction
518 of change, despite having lower RMSEP₁₀₀ and higher R² values than all other regional models (Table 3).
519 The eastern temperate forest (ETF) model most closely resembled the WA-Tol (inv) reconstruction at
520 both sites; this model had the highest number of samples and joint highest number of taxa of the eco-
521 region models (Table 3). Despite having a much lower R², and higher maximum and average bias values
522 (Table 3), the taiga reconstructions were broadly in line with the WA-Tol (inv) reconstruction at both
523 sites. The northern forest (NF) model reconstructions, despite being based on a high number of species
524 and taxa compared to most other eco-region models (Table 3), were variable in the extent to which they
525 aligned with other models. At Framboise, a site within the NF eco-region, the NF reconstruction was
526 closely aligned to the ETF and WA-Tol (inv) reconstructions, whereas at Lac Le Caron, it often exhibited
527 differing patterns and direction of change, suggesting potential problems with supra-regional
528 application of eco-region models (Turner et al., 2013). All eco-region model reconstructions at both sites
529 were tested for significance against models trained on random data (Telford and Birks, 2011b; Table 5).
530 *P* values for only two of ten reconstructions fell under the suggested significance cut-off value of 0.05
531 (NF and ETF models at Framboise, 0.015 and 0.007 respectively). Other *p* values ranged from 0.471 to
532 0.997 and no reconstructions at Lac Le Caron were significant. Taxa optima for the five eco-region
533 models were compared to those of the full dataset (Figure S7). Taxa optima rank, cf. Figure 8, was not
534 compared due to variable *n* for taxa in each eco-region model. Optima for individual taxa varied from
535 0.8 cm (*A. wrightianum*) to 42.5 cm (*Diffugia rubescens*), with a mean value of 11.6 cm and standard
536 deviation of 7.3 cm.

537

538 [INSERT FIGURE 7]

539 **Figure 7:** Comparison of transfer function reconstructions from five eco-region models. All panels
540 include comparison to pruned continental WA-Tol (inv) model. A and B are raw water table values (cm).
541 C and D are z-scores. A and C for Framboise bog, B and D for Lac Le Caron peatland. Model abbreviations
542 in key: NF = northern forests; NFM = northwestern forested mountains; MWCF = marine west coast
543 forest; ETF = eastern temperate forests. For all plots, higher y-axis water table depth or z-score values
544 indicate drier conditions. Note varying y-axis scales.

545

546 3.5. Combined North American and European compilation

547 Model development began with a dataset of 52 taxa and 3675 samples. Data pruning removed 250
548 samples with residual values >20% of the range of measured water table depths (19.4 cm). The pruned,
549 combined WA-Tol (inv) model (n = 3425) had an RMSEP_{LOO} of 7.94 cm and R² of 0.65, similar to
550 continental North American (RMSEP 7.42 cm, R² 0.72; Table 4) and European (RMSEP 7.72 cm, R² 0.59;
551 Amesbury et al., 2016) models, despite an almost doubling of sample numbers. Reconstructions using
552 North American, European (Amesbury et al., 2016) and combined models for independent palaeo
553 records in both Europe and North America were very similar when viewed as both reconstructed water
554 table depth values and z-scores (Figure 8). Individual taxa water table depth optima, whether in cm or
555 rank order, were not significantly different across the three models (comparing the European and North
556 American data as the only completely independent variables; for optima $r = 0.80$, $p < 0.05$, for rank $r_s =$
557 0.82 , $p < 0.05$), confirming WTD as an ecologically important environmental variable (cf. Juggins, 2013).
558 Despite the general consistency in WTD optima, some variability was evident. Most notably, *Diffflugia*
559 *labiosa* type was the wettest ranked taxa in the North American and combined models, with negative
560 values indicative of standing water, but ranked 45 of 46 taxa in the European model (Amesbury et al.,
561 2016) with a dry water table depth optima of ~25 cm. However, in the European dataset, *D. labiosa* was
562 only found in one sample in one eco-region (Scandinavia) at very low abundance (0.7%; Amesbury et
563 al., 2016) and was therefore poorly characterised. Its more extensive presence in the North American
564 dataset (as *D. oviformis* type) in 60 samples spanning two eco-regions (northern forests and eastern
565 temperate forests) with a maximum abundance of >50% provides better quality ecological data for this
566 taxon and highlights the value of large, ecologically diverse datasets in improving modern analogue
567 quality, as well as the persistent issue of taxonomic consistency (Payne et al., 2011). Other differences
568 in optima and rank were less extreme, but varied by up to 15 ranking positions or approximately 10 cm
569 in terms of water table optima (e.g. *Nebela penardiana* type, *Assulina seminulum* type). On average,
570 taxa optima varied by 4.3 cm and 5.2 ranking positions across all three models (equivalent values of 3.8
571 cm and 4.4 ranking positions excluding the anomalous *D. labiosa* type).

572

573 [INSERT FIGURES 8 AND 9]

574 **Figure 8:** Comparison of transfer function reconstructions from European, North American and
575 combined models. All models are pruned WA-Tol (inv). A and B are raw water table values (cm). C and
576 D are z-scores. A and C for Framboise, B and D for Tor Royal Bog. For all plots, higher y-axis water table
577 depth or z-score values indicate drier conditions. Note varying y-axis scales.

578

579 **Figure 9:** Comparison of water table depth optima (cm) for 46 taxa from European, North American and
580 combined models, ordered by the combined model. Top panel: rank order of taxa (coloured spots) with
581 range between highest and lowest rank (grey bars). Bottom panel: modelled optima (coloured spots)
582 with range between highest and lowest optima (grey bars). For references to colour, readers are
583 referred to the online version of the article.

584

585

586 **4. Discussion**

587

588 **4.1. A new continental-scale transfer function for North America**

589 Performance statistics (i.e. r^2 and $RMSEP_{L00}$) for the North American model were equivalent to a recent
590 European compilation (Amesbury et al., 2016) and a range of other regional-scale models within North
591 America and Europe (Table S7, i.e. within mean $\pm 1\sigma$ of 20 reviewed models). Further statistical tests
592 (*sensu*. Amesbury et al., 2013) showed that potential issues such as clustered sampling design and
593 spatial autocorrelation had only minimal effect on model performance and output. Reconstructions on
594 independent palaeo-data were comparable to a less sample-dense and more geographically restricted
595 North American model (Booth, 2008). Taken together, these multiple strands of evidence suggest that
596 our new model can be used as an effective tool to reconstruct peatland palaeohydrology throughout
597 the North American continent. More ecologically bespoke regional models may still provide reliable
598 reconstructions within and potentially even outside of their geographical limits (Turner et al., 2013;
599 Willis et al., 2015) and have an important role to play in ongoing research where they suit specific
600 research questions. However, the volume of data in the continental-scale compiled dataset provides
601 improved modern analogues for many taxa. All four models tested performed similarly in statistical
602 terms, however due to potential issues with spatial autocorrelation and the somewhat abrupt nature
603 of some reconstructed shifts in WTD with WMAT K5 and ML (Figure 6), as well as the differing magnitude
604 of ML reconstructions (Figure 6A and B), we favour WA-based models. A pruned WA-Tol (inv) model
605 marginally outperformed WAPLS C2 and produced reconstructions slightly more aligned to the model
606 of Booth (2008), so WA-Tol (inv) is our preferred model choice.

607

608 The variability of p values for significance testing of transfer function reconstructions (Telford and Birks,
609 2011b) between sites and models trained on the same data brings the use of the 'randomTF' test into
610 further question (Amesbury et al., 2016; Payne et al., 2016). Across all model types and eco-regions, no
611 reconstructions from Lac Le Caron had p values <0.05 . Eco-region model reconstructions for Framboise
612 varied widely between 0.007 and 0.782. At Framboise, NF and ETF model reconstructions were both
613 significant (0.015 and 0.007 respectively), whereas MWCF and taiga model reconstructions were non-
614 significant (0.471 and 0.485 respectively), despite showing extremely similar patterns of change (Figure
615 7; Table 5). Given that the efficacy of the 'randomTF' method has been recently reviewed and
616 questioned (Amesbury et al., 2016; Payne et al., 2016), these results further call into question the
617 usefulness of this test.

618

619 To make transfer functions more openly accessible to the research community and to facilitate users'
620 own application of the model to fossil data, we provide the full compiled North American dataset along
621 with R code to apply the WA-Tol (inv) model as supplementary information to this manuscript. In
622 addition, site-based datasets preserving the original taxonomy of the individual studies are available
623 through the Neotoma Paleoecological Database (www.neotomadb.org).

624

625 **4.2. North-American regional variability**

626 Biogeographical patterns that are evident in the dataset appear to be largely driven either by sampling
627 frequency or restricted to particular eco-regions (e.g. NFM). Outside of these limitations,
628 biogeographical differences occurred against a background of relative cosmopolitanism across the
629 dataset. For example, the finding that *H. papilio* occurred across all eco-regions is particularly interesting
630 given recent evidence suggesting that it displays geographical patterns of both genotypic and
631 phenotypic diversity in other regions (Heger et al., 2013; Amesbury et al., 2016). This observation is
632 reassuring for the broader applicability of transfer functions across large geographical areas. Although
633 we used only a moderate taxonomic resolution (higher than for a European compilation; Amesbury et
634 al., 2016) that did not allow us to identify the full complexity of biogeographic patterns, and hence may

635 have caused us to miss some discrepancies in taxa hydrological optima, this potential loss of information
636 did not result in poor model performance. Even though a higher taxonomic resolution may permit the
637 development of more precise transfer function models it appears that the taxonomic scheme currently
638 used by ecologists and palaeoecologists is robust and the resulting model performance satisfactory.

639
640 Taxa optima were broadly consistent across eco-region models (Figure S7), with mean variability
641 between eco-region models of 11.6 cm. Highly variable water table depth optima for individual taxa
642 tended to be driven by poor characterisation. For example, *Diffflugia rubescens* and *Arcella gibbosa* both
643 had tightly clustered optima across a majority of models, with outlying values for the MCWF model only
644 driving the two highest values for overall optima range; in that model, the optima for both taxa were
645 driven by occurrence in a single sample (from 191 samples in the model; Table 3), both at <2%. Likewise,
646 the outlying optima for *Padaungiella lageniformis* in the NF model was driven by only 6 occurrences
647 (from 915 samples in the model; Table 3), never at >1% abundance. Thus, whilst the variability evident
648 between taxa optima across eco-regions may be partly driven by genuine biogeographical differences,
649 the overall consistency provides support for continental-scale compilation. The variability in eco-region
650 model reconstructions illustrates a potential advantage of sample dense continental-scale compilations.
651 In particular, the NFM model produced anomalous reconstructions that were significantly drier (i.e.
652 higher WTD) than other eco-region models and also anomalous when viewed as z-scores. Although not
653 clearly outlying and therefore included in the data analysis, this was the only region to be partly
654 clustered in the NMDS analysis (section 3.1) and was relatively taxa poor. All sites in this eco-region
655 were from the Rocky Mountains and, although *Sphagnum*-dominated, were typically fens and included
656 sites that were fed by highly acidic and iron-rich groundwater (Booth and Zygmunt, 2005), which
657 appears to have driven a distinct local flora. Although this produced anomalous results for a regional-
658 scale model, when these data were included in a continental-scale model, potentially confounding
659 factors did not overtly effect the magnitude or direction of change of the reconstruction (Figure 7),
660 whilst valuable ecological information was maintained.

661
662 **4.3. Spatial scales for transfer function development**
663 Continental-scale models from North America and Europe, as well as a combined model, reconstructed
664 independent test data from both continents identically, in terms of palaeohydrological interpretation.
665 Despite some variability, water table depth optima were also broadly aligned between continents
666 (Figure 9). Modelled water table depth optima and taxa distribution may vary on local or regional scales
667 due to differences in peatland type (e.g. forested vs. non-forested; Beaulne et al., 2018), climatic context
668 (Booth and Zygmunt, 2005) or the influence of non-linear processes such as permafrost (e.g. at the
669 unpublished Scotty Creek and Toolik sites (Table 1); see also Lamarre et al., 2013). However, the relative
670 position and ecological niches of taxa in respect to surface wetness is often more consistent (Booth and
671 Zygmunt, 2005; Beaulne et al., 2018). Our comparison of water table depth optima and rank between
672 European and North American compilations showed that, with the exception of a single anomalous
673 taxon, differences were relatively small (Figure 9) and importantly, did not have a noticeable effect on
674 reconstructions of test data from both within and outside of each continent, especially when viewed as
675 residual values (Figure 8; Swindles et al., 2015a). Therefore, it appears that potentially confounding
676 climatic or peatland type differences that may exist within continental-scale compiled datasets are
677 compensated by more in-depth characterisation of the average ecological niche of each taxon.

678
679 These findings also support the recent assertion that transfer functions trained on very large datasets
680 perform well due to the vastly increased number of analogues contained within them, which provide a
681 better representation of testate amoeba ecology than less populated local- or regional-scale models
682 where modern analogues may be either lacking or based on low numbers of samples for some taxa
683 (Amesbury et al., 2016). In a test of regional and supra-regional application of transfer functions, the

684 only difference between reconstructions was in the absolute magnitude of change (i.e. in reconstructed
685 water table depth values), with direction of change, the most reliable variable for palaeoclimatic
686 interpretation, consistent (Turner et al., 2013; Swindles et al., 2015a). Given that the recent suggestion
687 to display transfer function output as standardised z-scores (Swindles et al., 2015a; Amesbury et al.,
688 2016) tends to mitigate magnitude differences, we therefore advocate the further development and
689 use of continental-scale models that maximise modern analogue quality without losing reconstructive
690 skill and provide standard reconstruction tools with directly comparable results.

691
692 Continental-scale models from North America (this study) and Europe (Amesbury et al., 2016) have
693 similar performance statistics than regional- or local-scale models, but potentially offer additional
694 scientific benefit. The compilation and taxonomic harmonisation of such datasets, alongside their
695 archiving in freely available repositories (e.g. Neotoma), permits further community-driven effort
696 towards a better understanding of wide-scale testate amoeba ecology and biogeography that can
697 contextualise and enhance the interpretation of transfer function results. In addition, the lack of
698 significant reduction in performance statistics and similarity of reconstructions produced by a combined
699 North American and European model, when compared to the two continental-scale models suggests
700 that any geographical limit of scale beyond which further compilation of peatland testate amoebae data
701 would not be beneficial, has not yet been reached. We therefore call for the continued synthesis of
702 modern testate amoeba data, particularly for Eurasia. Our results show that harmonisation of this data
703 alongside existing datasets may permit a future Holarctic synthesis of peatland testate amoeba ecology
704 and biogeography. A potential challenge when extending beyond the Holarctic realm is that additional
705 Southern Hemisphere specific taxa (e.g. *Alocodera*, *Apodera*, *Certesella*) will need to be considered,
706 while many characteristic taxa of northern peatlands will be missing (e.g. *Planocarina*, *Hyalosphenia*
707 *papilio*).

708 709 **5. Conclusions**

710 We compiled a dataset of 1956 modern surface testate amoeba samples from 137 peatlands located
711 throughout the United States of America and Canada. Following data management procedures, a
712 reduced dataset of 1927 samples was used, following exploratory NMDS analysis, to develop
713 continental-scale transfer function models. These models were tested using a range of statistical
714 approaches and application to independent palaeo-data. Though all pruned models tested were valid,
715 WA-Tol (inv) was selected as our preferred model choice. Our new model provides an effective,
716 standardised tool for reconstructing peatland palaeohydrology throughout the North American
717 continent. Using the compiled dataset and models based on EPA Level 1 eco-regions, we examined
718 regional variability within the dataset. Some regions and taxa demonstrated differences in taxonomic
719 diversity and/or biogeography, but these were set against a broad pattern of cosmopolitanism across
720 the dataset. To examine the potential for a future Holarctic synthesis of peatland testate amoeba data,
721 we combined our new North American dataset with an existing recent compilation from Europe to form
722 a combined dataset of >3700 samples. Model outputs from this compilation were equivalent to the
723 North American and European models independently, suggesting that there is scope for further merging
724 of data to develop a future Holarctic dataset and transfer function. Such a dataset would be an
725 extremely valuable community resource, allowing collaborative examination of peatland testate
726 amoeba ecological and biogeographical patterns to an extent not currently possible.

727 728 **Acknowledgements**

729 We gratefully acknowledge and thank the many landowners and data collectors that have helped to
730 facilitate the many fieldwork campaigns that eventually led to our new database of North American
731 testate amoebae, but who are too numerous to list individually here. Compilation of the individual
732 datasets and their submission to the Neotoma Paleoecology Database was supported by EAR-1550716

733 under the guidance of RKB. RKB was also funded by the National Science Foundation (EAR-0902441,
734 ATM-0625298) and the United State Geological Survey (USGS-DOI cooperative agreement
735 06ERAG0019). MJA, DJC, PDMH and HM were funded by the UK Natural Environment Research Council
736 (grants NE/G019851/1, NE/G020272/1, NE/G019673/1 and NE/G02006X/1). HM was also funded by a
737 UK Quaternary Research Association New Research Workers' Award. RJP was funded by the Russian
738 Science Foundation (grant 14-14-00891). EADM was funded by the University of Alaska Anchorage and
739 the Swiss National Science Foundation (grants 205321-109709/1 and 205321-109709/2). JT and NP
740 were funded by the National Sciences and Engineering Research Council of Canada (grant No: 2014-
741 05878)

742

743 **References**

744 Amesbury, M.J., Mallon, G., Charman, D.J., Hughes, P.D.M., Booth, R.K., Daley, T.J., Garneau, M., 2013.
745 Statistical testing of a new testate amoeba-based transfer function for water-table depth reconstruction
746 on ombrotrophic peatlands in north-eastern Canada and Maine, United States. *J. Quat. Sci.* 28, 27–39.

747 Amesbury, M.J., Swindles, G.T., Bobrov, A., Charman, D.J., Holden, J., Lamentowicz, M., Mallon, G.,
748 Mazei, Y.A., Mitchell, E.A.D., Payne, R.J., Roland, T.P., Turner, T.E., Warner, B.G., 2016. Development of
749 a new pan-European testate amoeba transfer function for reconstructing peatland palaeohydrology.
750 *Quat. Sci. Rev.* 152, 132–151.

751 Baas Becking, L.G.M., 1934. *Geobiologie of Inleiding tot de Milieukunde*. The Hague: Van Stockum &
752 Zoon.

753 Beaulne, J., Magnan, G., Garneau, M., 2018. Evaluating the potential of testate amoebae as indicators
754 of hydrological conditions in boreal forested peatlands. *Ecol. Indic.* 91, 386–394.

755 Beyens, L., Bobrov, A., 2016. Evidence supporting the concept of a regionalized distribution of testate
756 amoebae in the Arctic. *Acta Protozool.* 55, 197–209.

757 **Bobrov, A.A., Charman, D.J., Warner, B.G., 1999. Ecology of testate amoebae (Protozoa: Rhizopoda)**
758 **on peatlands in western Russia with special attention to niche separation in closely related taxa.**
759 ***Protist* 150, 125–136.**

760 Booth, R.K., 2001. Ecology of testate amoebae (Protozoa) in two Lake Superior coastal wetlands:
761 implications for paleoecology and environmental monitoring. *Wetlands* 21, 564–576.

762 Booth, R.K., 2002. Testate amoebae as paleoindicators of surface-moisture changes on Michigan
763 peatlands : modern ecology and hydrological calibration. *J. Paleolimnol.* 28, 329–348.

764 Booth, R.K., 2008. Testate amoebae as proxies for mean annual water-table depth in Sphagnum-
765 dominated peatlands of North America. *J. Quat. Sci.* 23, 43–57.

766 Booth, R.K., Sullivan, M.E., Sousa, V.A., 2008. Ecology of testate amoebae in a North Carolina pocosin
767 and their potential use as environmental and paleoenvironmental indicators. *Écoscience* 15, 277–289.

768 Booth, R.K., Zygmunt, J.R., 2005. Biogeography and comparative ecology of testate amoebae inhabiting
769 Sphagnum-dominated peatlands in the Great Lakes and Rocky Mountain regions of North America.
770 *Divers. Distrib.* 11, 577–590.

771 Charman, D.J., Warner, B.G., 1997. The ecology of testate amoebae (Protozoa: Rhizopoda) in oceanic
772 peatlands in Newfoundland, Canada: Modelling hydrological relationships for palaeoenvironmental
773 reconstruction. *Écoscience* 4, 555–562.

774 Charman, D.J., Blundell, A., ACCROTELM Members, 2007. A new European testate amoebae transfer
775 function for palaeohydrological reconstruction on ombrotrophic peatlands. *J. Quat. Sci.* 22, 209–221.

- 776 Charman, D.J., Warner, B.G., 1992. Relationship between testate amoebae (Protozoa: Rhizopoda) and
777 microenvironmental parameters on a forested peatland in northeastern Ontario. *Can. J. Zool.* 70, 2474–
778 2482.
- 779 De Wit, R., Bouvier, T., 2006. “Everything is everywhere, but, the environment selects”; what did Baas
780 Becking and Beijerinck really say? *Environ. Microbiol.* 8, 755–758.
- 781 Duckert, C., Blandenier, Q., Kupferschmid, F.A.L., Kosakyan, A., Mitchell, E.A.D., Lara, E., Singer, D.
782 2018 in press. En garde! Redefinition of *Nebela militaris* (Arcellindia, Hyalospheniidae) and erection of
783 *Alabasta* gen. nov. *Eur. J. Protistol.*
- 784 Fernández, L.D., Fournier, B., Rivera, R., Lara, E., Mitchell, E.A.D., Hernández, C.E., 2016. Water–energy
785 balance, past ecological perturbations and evolutionary constraints shape the latitudinal diversity
786 gradient of soil testate amoebae in south-western South America. *Glob. Ecol. Biogeogr.* 25, 1216–1227.
- 787 Foissner, W., 2006. Biogeography and dispersal of micro-organisms: A review emphasizing protists. *Acta*
788 *Proto* 45, 111–136.
- 789 Foissner, W., 2008. Protist diversity and distribution: some basic considerations. *Biodivers. Conserv.* 17,
790 235–242.
- 791 Fournier, B., Coffey, E.E.D., van der Knaap, W.O., Fernández, L.D., Bobrov, A., Mitchell, E.A.D., 2015. A
792 legacy of human-induced ecosystem changes: Spatial processes drive the taxonomic and functional
793 diversities of testate amoebae in Sphagnum peatlands of the Galápagos. *J. Biogeogr.* 43, 533–543.
- 794 Geisen, S., Mitchell, E.A.D., Wilkinson, D.M., Adl, S., Bonkowski, M., Brown, M.W., Fiore-Donno, A.M.,
795 Heger, T.J., Jasey, V.E.J., Krashevskaya, V., Lahr, D.J.G., Marcisz, K., Mulot, M., Payne, R., Singer, D.,
796 Anderson, O.R., Charman, D.J., Ekelund, F., Griffiths, B.S., Rønn, R., Smirnov, A., Bass, D., Belbahri, L.,
797 Berney, C., Blandenier, Q., Chatzinotas, A., Clarholm, M., Dunthorn, M., Feest, A., Fernández, L.D.,
798 Foissner, W., Fournier, B., Gentekaki, E., Hájek, M., Helder, J., Jousset, A., Koller, R., Kumar, S., La Terza,
799 A., Lamentowicz, M., Mazei, Y., Santos, S.S., Seppey, C.V.W., Spiegel, F.W., Walochnik, J., Winding, A.,
800 Lara, E., 2017. Soil protistology rebooted: 30 fundamental questions to start with. *Soil Biol. Biochem.*
801 111, 94–103.
- 802 Hammer, Ø., Harper, D.A.T., Ryan, P.D., 2001. PAST: paleontological statistics software package for
803 education and data analysis. *Palaeontol. Electron.* 4, 9pp. [http://palaeo-](http://palaeo-electronica.org/2001_1/past/issue1_01.htm)
804 [electronica.org/2001_1/past/issue1_01.htm](http://palaeo-electronica.org/2001_1/past/issue1_01.htm).
- 805 Heger, T.J., Mitchell, E.A.D., Leander, B.S., 2013. Holarctic phylogeography of the testate amoeba
806 *Hyalosphenia papilio* (Amoebozoa: Arcellinida) reveals extensive genetic diversity explained more by
807 environment than dispersal limitation. *Mol. Ecol.* 22, 5172–5184.
- 808 Juggins, S., 2013. Quantitative reconstructions in palaeolimnology: New paradigm or sick science? *Quat.*
809 *Sci. Rev.* 64, 20–32.
- 810 Juggins, S., 2015. Rioja: Analysis of Quaternary Science Data. R Package Version 0.9-5. [https://cran.r-](https://cran.r-project.org/web/packages/rioja/index.html)
811 [project.org/web/packages/rioja/index.html](https://cran.r-project.org/web/packages/rioja/index.html).
- 812 Kosakyan, A., Lahr, D.J.G., Mulot, M., Meisterfeld, R., Edward, A., Mitchell, D., Lara, E., 2016.
813 Phylogenetic reconstruction based on COI reshuffles the taxonomy of hyalosphenid shelled testate
814 amoebae and reveals the convoluted evolution of shell plate shapes. *Cladistics* 32, 606–623.
- 815 Laggoun-Défarge, F., Mitchell, E., Gilbert, D., Disnar, J.R., Comont, L., Warner, B.G., Buttler, A., 2008.
816 Cut-over peatland regeneration assessment using organic matter and microbial indicators (bacteria and
817 testate amoebae). *J. Appl. Ecol.* 45, 716–727.

- 818 Lamarre, A., Garneau, M., Asnong, H., 2012. Holocene paleohydrological reconstruction and carbon
819 accumulation of a permafrost peatland using testate amoeba and macrofossil analyses, Kuujjuarapik,
820 subarctic Québec, Canada. *Rev. Palaeobot. Palynol.* 186, 131–141.
- 821 Lamarre, A., Magnan, G., Garneau, M., Boucher, É., 2013. A testate amoeba-based transfer function for
822 paleohydrological reconstruction from boreal and subarctic peatlands in northeastern Canada. *Quat.*
823 *Int.* 306, 88–96.
- 824 Lamentowicz, L., Lamentowicz, M., Gałka, M., 2008. Testate amoebae ecology and a local transfer
825 function from a peatland in western Poland. *Wetlands* 28, 164–175.
- 826 Lamentowicz, M., Mitchell, E.A.D., 2005. The ecology of testate amoebae (protists) in *Sphagnum* in
827 north-western Poland in relation to peatland ecology. *Microb. Ecol.* 50, 48–63.
- 828 Lara, E., Roussel-Delif, L., Fournier, B., Wilkinson, D.M., Mitchell, E.A.D., 2016. Soil microorganisms
829 behave like macroscopic organisms: patterns in the global distribution of soil euglyphid testate
830 amoebae. *J. Biogeogr.* 43, 520–532.
- 831 Li, H., Wang, S., Zhao, H., Wang, M., 2015. A testate amoebae transfer function from *Sphagnum*-
832 dominated peatlands in the Lesser Khingan Mountains, NE China. *J. Paleolimnol.* 54, 189–203.
- 833 Magnan, G., Garneau, M., 2014. Evaluating long-term regional climate variability in the maritime region
834 of the St. Lawrence North Shore (eastern Canada) using a multi-site comparison of peat-based
835 paleohydrological records. *J. Quat. Sci.* 29, 209–220.
- 836 Marcisz, K., Lamentowicz, Ł., Słowińska, S., Słowiński, M., Muszak, W., Lamentowicz, M., 2014. Seasonal
837 changes in *Sphagnum* peatland testate amoeba communities along a hydrological gradient. *Eur. J.*
838 *Protistol.* 50, 445–455.
- 839 Markel, E.R., Booth, R.K., Yangmin Qin, 2010. Testate amoebae and ^{13}C of *Sphagnum* as surface-
840 moisture proxies in Alaskan peatlands. *The Holocene* 20, 463–475.
- 841 Mitchell, E.A.D., Charman, D.J., Warner, B.G., 2008. Testate amoebae analysis in ecological and
842 paleoecological studies of wetlands: Past, present and future. *Biodivers. Conserv.* 17, 2115–2137.
- 843 Oliverio, A.M., Lahr, D.J.G., Nguyen, T., Katz, L. a., 2014. Cryptic diversity within morphospecies of
844 testate amoebae (Amoebozoa: Arcellinida) in New England bogs and fens. *Protist* 165, 196–207.
- 845 O'Malley, M.A., 2008. "Everything is everywhere: but the environment selects": ubiquitous distribution
846 and ecological determinism in microbial biogeography. *Stud. Hist. Philos. Sci. Part C Stud. Hist. Philos.*
847 *Biol. Biomed. Sci.* 39, 314–325.
- 848 O'Malley, M.A., 2007. The nineteenth century roots of "everything is everywhere." *Nat. Rev. Microbiol.*
849 5, 647–651.
- 850 Oksanen, J., Blanchet, F.G., Kindt, R., Legendre, P., Minchin, P.R., Hara, R.B.O., Simpson, G.L., Solymos,
851 P., Stevens, M.H.H., Wagner, H., 2015. Package "vegan" version 2.3-1.
- 852 Payne, R.J., Babeshko, K. V., van Bellen, S., Blackford, J.J., Booth, R.K., Charman, D.J., Ellershaw, M.R.,
853 Gilbert, D., Hughes, P.D.M., Jassey, V.E.J., Lamentowicz, L., Lamentowicz, M., Malysheva, E.A., Mauquoy,
854 D., Mazei, Y.A., Mitchell, E.A.D., Swindles, G.T., Tsyganov, A., Turner, T.E., Telford, R.J., 2016. Significance
855 testing testate amoeba water table reconstructions. *Quat. Sci. Rev.* 138, 131–135.
- 856 Payne, R.J., Kishaba, K., Blackford, J.J., Mitchell, E.A.D., 2006. Ecology of testate amoebae (Protista) in
857 south-central Alaska peatlands: building transfer-function models for palaeoenvironmental studies. *The*
858 *Holocene* 16, 403–414.

859 Payne, R.J., Mitchell, E.A.D., 2007. Ecology of Testate Amoebae from Mires in the Central Rhodope
860 Mountains, Greece and Development of a Transfer Function for Palaeohydrological Reconstruction.
861 *Protist* 158, 159–171.

862 Payne, R.J., Charman, D.J., Matthews, S., Eastwood, W.J., 2008. Testate amoebae as
863 palaeohydrological proxies in Sürmene Ağaçbaşı Yaylasi peatland (northeast Turkey). *Wetlands* 28,
864 311–323.

865 Payne, R.J., Ryan, P.A., Nishri, A., Gophen, M., 2010. Testate amoeba communities of the drained Hula
866 wetland (Israel): Implications for ecosystem development and conservation management. *Wetl. Ecol.*
867 *Manag.* 18, 177–189.

868 Payne, R.J., Lamentowicz, M., Mitchell, E.A.D., 2011. The perils of taxonomic inconsistency in
869 quantitative palaeoecology: Experiments with testate amoeba data. *Boreas* 40, 15–27.

870 Payne, R.J., Telford, R.J., Blackford, J.J., Blundell, A., Booth, R.K., Charman, D.J., Lamentowicz, M.,
871 Mitchell, E.A.D., Potts, G., Swindles, G.T., Warner, B.G., Lamentowicz, L., Woodland, W.A., 2012. Testing
872 peatland testate amoeba transfer for clustered training-sets. *The Holocene* 22, 819–825.

873 Pelletier, N., Talbot, J., Olefeldt, D., Turetsky, M.R., Blodau, C., Sonnentag, O., Quinton, W.L., 2017.
874 Influence of Holocene permafrost aggradation and thaw on the paleoecology and carbon storage of a
875 peatland complex in northwestern Canada. *The Holocene* 27, 1391–1405.

876 Pérez-Juárez, H., Serrano-Vázquez, A., Kosakyan, A., Mitchell, E.A.D., Rivera Aguilar, V.M., Lahr, D.J.G.,
877 Hernández Moreno, M.M., Cuellar, H.M., Eguiarte, L.E., Lara, E., 2017. *Quadrulella texcalense* sp. nov.
878 from a Mexican desert: An unexpected new environment for hyalospheniid testate amoebae. *Eur. J.*
879 *Protistol.* 61, 253–264.

880 Reczuga, M.K., Swindles, G.T., Grewling, Ł., Lamentowicz, M., 2015. *Arcella peruviana* sp. nov.
881 (Amoebozoa: Arcellinida, Arcellidae), a new species from a tropical peatland in Amazonia. *Eur. J.*
882 *Protistol.* 51, 437–449.

883 Roe, H.M., Elliott, S.M., Patterson, R.T., 2017. Re-assessing the vertical distribution of testate amoeba
884 communities in surface peats: implications for palaeohydrological studies. *Eur. J. Protistol.*

885 Roland, T.P., Amesbury, M.J., Wilkinson, D.M., Charman, D.J., Convey, P., Hodgson, D.A., Royles, J.,
886 Clauß, S., Völcker, E., 2017. Taxonomic implications of morphological complexity within the testate
887 amoeba genus *Corythion* from the Antarctic Peninsula. *Protist* 168, 565–585.

888 Singer, D., Kosakyan, A., Seppey, C.V.W., Pillonel, A., Fernández, L.D., Fontaneto, D., Mitchell, E.A.D.,
889 Lara, E., 2018. Environmental filtering and phylogenetic clustering correlate with the distribution
890 patterns of cryptic protist species. *Ecology* 99, 904–914.

891 Smith, H.G., Bobrov, A., Lara, E., 2008. Diversity and biogeography of testate amoebae. *Biodivers.*
892 *Conserv.* 17, 329–343.

893 Smith, H.G., Wilkinson, D.M., 2007. Not all free-living microorganisms have cosmopolitan distributions
894 – the case of *Nebela* (Apodera) *vas Certes* (Protozoa : Amoebozoa : Arcellinida). *J. Biogeog.* 34, 1822–
895 1831.

896 Sullivan, M.E., Booth, R.K., 2011. The potential influence of short-term environmental variability on the
897 composition of testate amoeba communities in Sphagnum peatlands. *Microb. Ecol.* 62, 80–93.

898 Swindles, G.T., Charman, D.J., Roe, H.M., Sansum, P.A., 2009. Environmental controls on peatland
899 testate amoebae (Protozoa: Rhizopoda) in the North of Ireland: Implications for Holocene palaeoclimate
900 studies. *J. Paleolimnol.* 42, 123–140.

901 Swindles, G.T., Lawson, I.T., Matthews, I.P., Blaauw, M., Daley, T.J., Charman, D.J., Roland, T.P., Plunkett,
902 G.M., Schettler, G., Gearey, B.R., Turner, T.E., Rea, H.A., Roe, H.M., Amesbury, M.J., Chambers, F.M.,
903 Holmes, J., Mitchell, F.J.G., Blackford, J.J., Blundell, A., Branch, N., Holmes, J., Langdon, P.G., McCarroll,
904 J., McDermott, F., Oksanen, P.O., Pritchard, O., Stastney, P., Stefanini, B., Young, D., Wheeler, J., Becker,
905 K., 2013. Centennial-scale climate change in Ireland during the Holocene. *Earth-Science Rev.* 126, 300–
906 320.

907 Swindles, G.T., Reczuga, M., Lamentowicz, M., Raby, C.L., Turner, T.E., Charman, D.J., Gallego-Sala, A.,
908 Valderrama, E., Williams, C., Draper, F., Honorio Coronado, E.N., Roucoux, K.H., Baker, T., Mullan, D.J.,
909 2014. Ecology of testate amoebae in an Amazonian peatland and development of a transfer function
910 for palaeohydrological reconstruction. *Microb. Ecol.* 68, 284–298.

911 Swindles, G.T., Holden, J., Raby, C.L., Turner, T.E., Blundell, A., Charman, D.J., Menberu, M.W., Kløve, B.,
912 2015a. Testing peatland water-table depth transfer functions using high-resolution hydrological
913 monitoring data. *Quat. Sci. Rev.* 120, 107–117.

914 Swindles, G.T., Morris, P.J., Mullan, D., Watson, E.J., Turner, T.E., Roland, T.P., Amesbury, M.J., Kokfelt,
915 U., Schoning, K., Pratte, S., Gallego-Sala, A., Charman, D.J., Sanderson, N., Garneau, M., Carrivick, J.,
916 Woulds, C., Holden, J., Parry, L., Galloway, J.M., 2015b. The long-term fate of permafrost peatlands
917 under rapid climate warming. *Nat. Sci. Reports.* 5:17951. doi: 10.1038/srep17951.

918 Swindles, G.T., Amesbury, M.J., Turner, T.E., Carrivick, J.L., Woulds, C., Raby, C.L., Mullan, D.J., Roland,
919 T.P., Galloway, J.M., Parry, L.E., Kokfelt, U., Garneau, M., Charman, D.J., Holden, J., 2015c. Evaluating
920 the use of testate amoebae for palaeohydrological reconstruction in permafrost peatlands.
921 *Palaeogeogr. Palaeoclimatol. Palaeoecol.* 424, 111–122.

922 Talbot, J., Richard, P.J.H., Roulet, N.T., Booth, R.K., 2010. Assessing long-term hydrological and ecological
923 responses to drainage in a raised bog using paleoecology and a hydrosequence. *J. Veg. Sci.* 21, 143–156.

924 Telford, R.J., Birks, H.J.B., 2005. The secret assumption of transfer functions: Problems with spatial
925 autocorrelation in evaluating model performance. *Quat. Sci. Rev.* 24, 2173–2179.

926 Telford, R.J., Birks, H.J.B., 2009. Evaluation of transfer functions in spatially structured environments.
927 *Quat. Sci. Rev.* 28, 1309–1316.

928 Telford, R.J., Birks, H.J.B., 2011a. Effect of uneven sampling along an environmental gradient on transfer-
929 function performance. *J. Paleolimnol.* 46, 99–106.

930 Telford, R.J., Birks, H.J.B., 2011b. A novel method for assessing the statistical significance of quantitative
931 reconstructions inferred from biotic assemblages. *Quat. Sci. Rev.* 30, 1272–1278.

932 Telford, R.J., 2015. palaeoSig: Significance Tests for Palaeoenvironmental Reconstructions. R Package
933 Version 1.1-3. <https://cran.r-project.org/web/packages/palaeoSig/>.

934 Turner, T.E., Swindles, G.T., Charman, D.J., Blundell, A., 2013. Comparing regional and supra-regional
935 transfer functions for palaeohydrological reconstruction from Holocene peatlands. *Palaeogeogr.*
936 *Palaeoclimatol. Palaeoecol.* 369, 395–408.

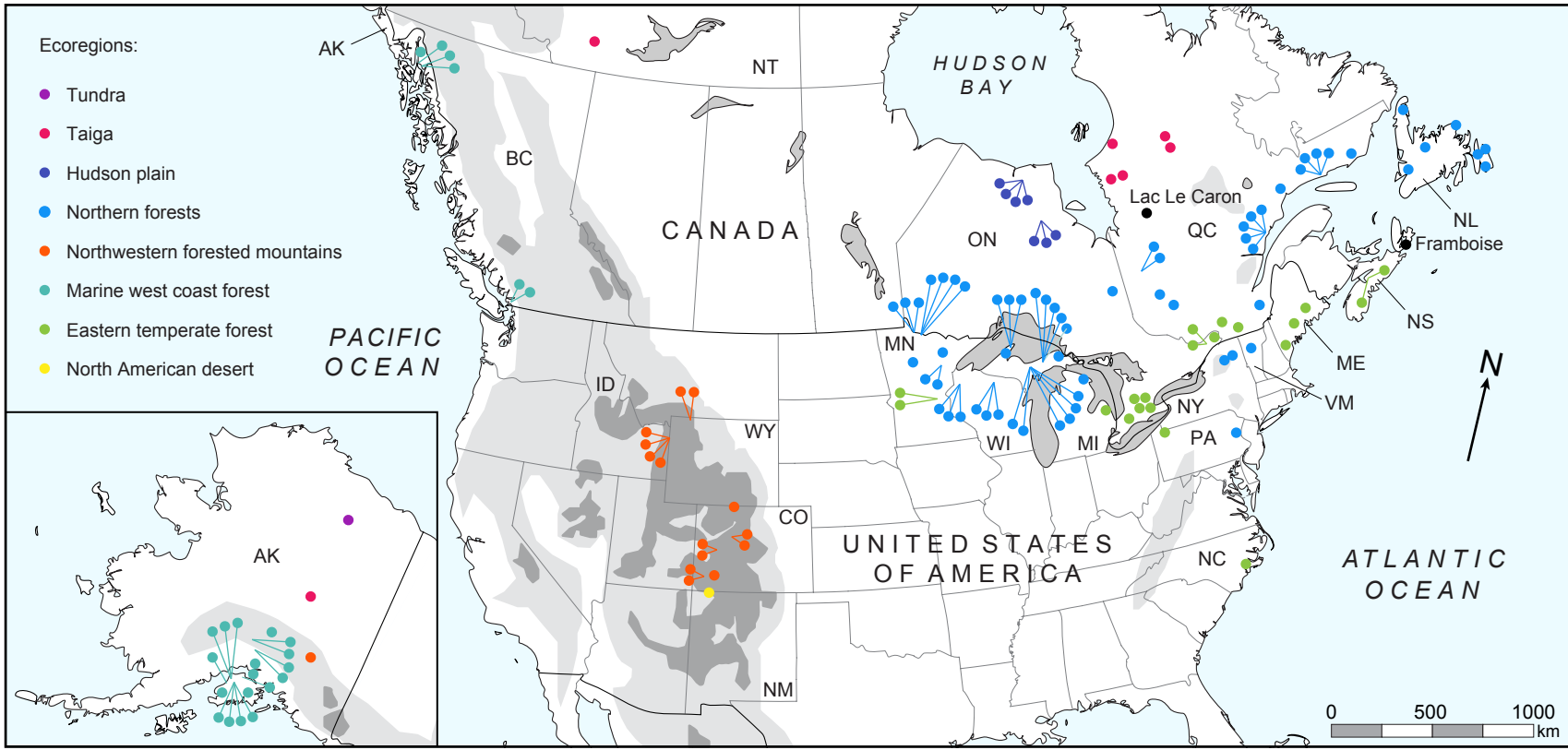
937 van Bellen, S., Garneau, M., Booth, R.K., 2011. Holocene carbon accumulation rates from three
938 ombrotrophic peatlands in boreal Quebec, Canada: Impact of climate-driven ecohydrological change.
939 *Holocene* 21, 1217–1231.

940 van Bellen, S., Mauquoy, D., Payne, R.J., Roland, T.P., Daley, T.J., Hughes, P.D.M., Loader, N.J., Street-
941 Perrott, F.A., Rice, E.M., Pancotto, V. a., Bellen, S.V.A.N., 2014. Testate amoebae as a proxy for
942 reconstructing Holocene water table dynamics in southern Patagonian peat bogs. *J. Quat. Sci.* 29, 463–
943 474.

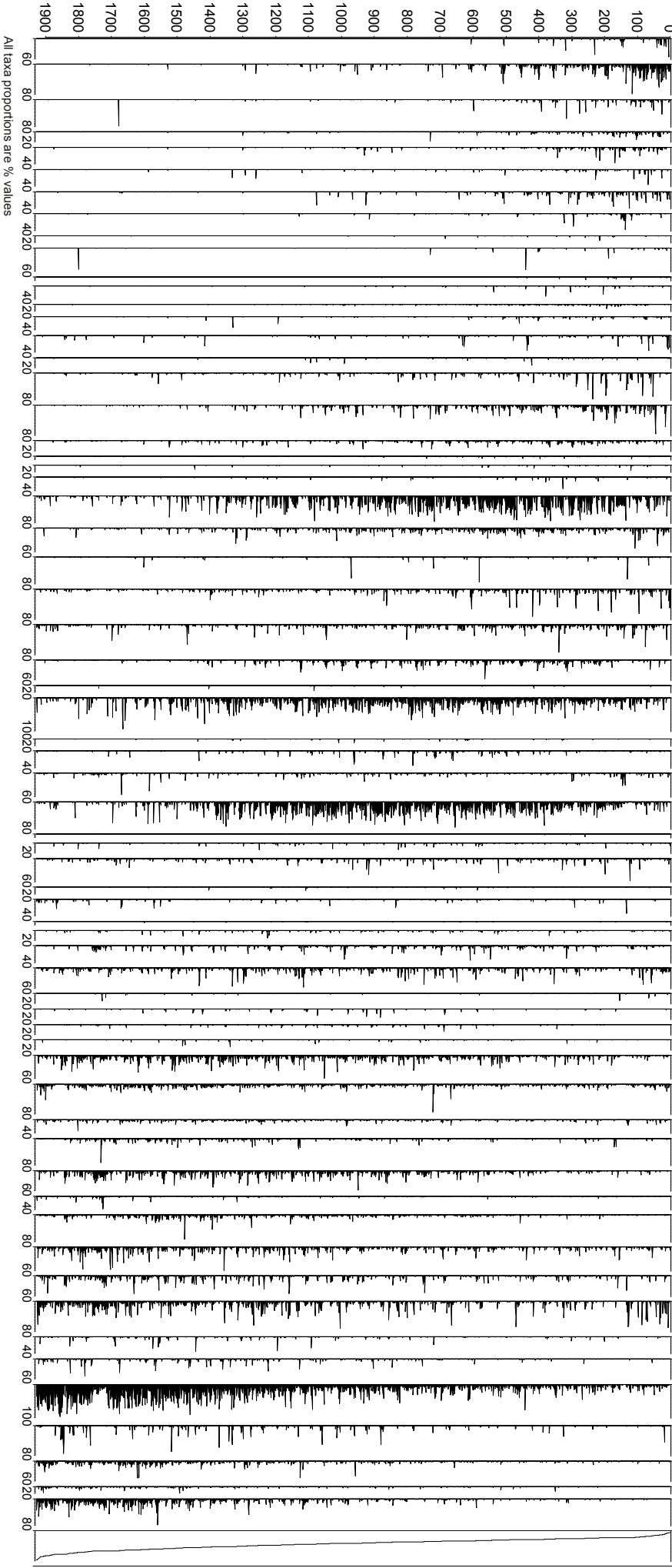
- 944 van Bellen, S., Mauquoy, D., Hughes, P.D., Roland, T.P., Daley, T.J., Loader, N.J., Street-Perrott, F.A., Rice,
945 E.M., Pancotto, V.A., Payne, R.J., 2016. Late-Holocene climate dynamics recorded in the peat bogs of
946 Tierra del Fuego, South America. *The Holocene* 26, 489–501.
- 947 Warner, B.G., 1987. Abundance and Diversity of Testate Amoebae (Rhizopoda, Testacea) in Sphagnum
948 Peatlands in Southwestern Ontario, Canada. *Arch. fur Protistenkd.* 133, 173–189.
- 949 Warner, B.G., Charman, D.J., 1994. Holocene changes on a peatland in northwestern Ontario
950 interpreted from testate amoebae (Protozoa) analysis. *Boreas* 23, 270–279.
- 951 Willis, K.S., Beilman, D., Booth, R.K., Amesbury, M.J., Holmquist, J., MacDonald, G., 2015. Peatland
952 paleohydrology in southern West Siberian Lowlands: Comparison of multiple testate amoeba transfer
953 functions, sites, and Sphagnum ¹³C values. *The Holocene* 25, 1425–1436.
- 954 **Woodland, W.A., Charman, D.J., Sims, P.C., 1998. Quantitative estimates of water tables and soil
955 moisture in Holocene peatlands from testate amoebae. *The Holocene* 8, 261–273.**
- 956 Zhang, H., Piilo, S.R., Amesbury, M.J., Charman, D.J., Gallego-Sala, A. V., Väiliranta, M.M., 2018. The
957 role of climate change in regulating Arctic permafrost peatland hydrological and vegetation change
958 over the last millennium. *Quat. Sci. Rev.* 182, 121–130.

Ecoregions:

- Tundra
- Taiga
- Hudson plain
- Northern forests
- Northwestern forested mountains
- Marine west coast forest
- Eastern temperate forest
- North American desert



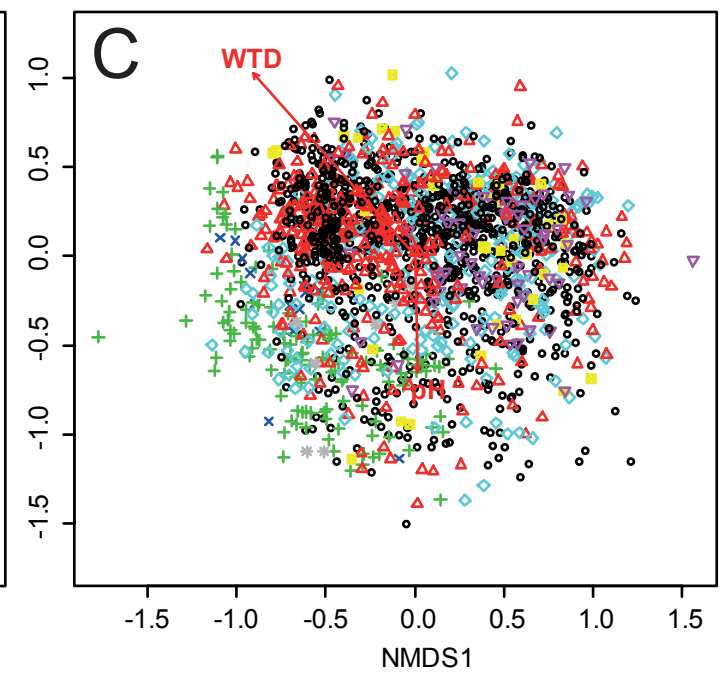
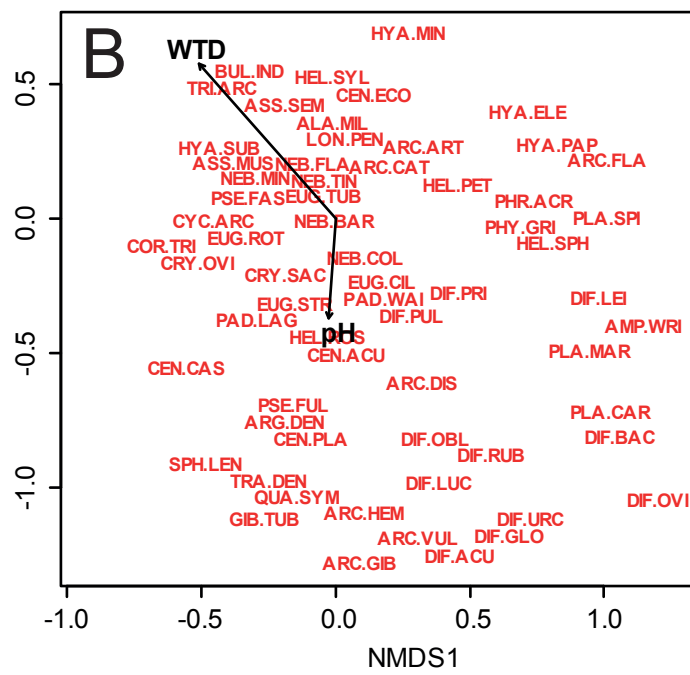
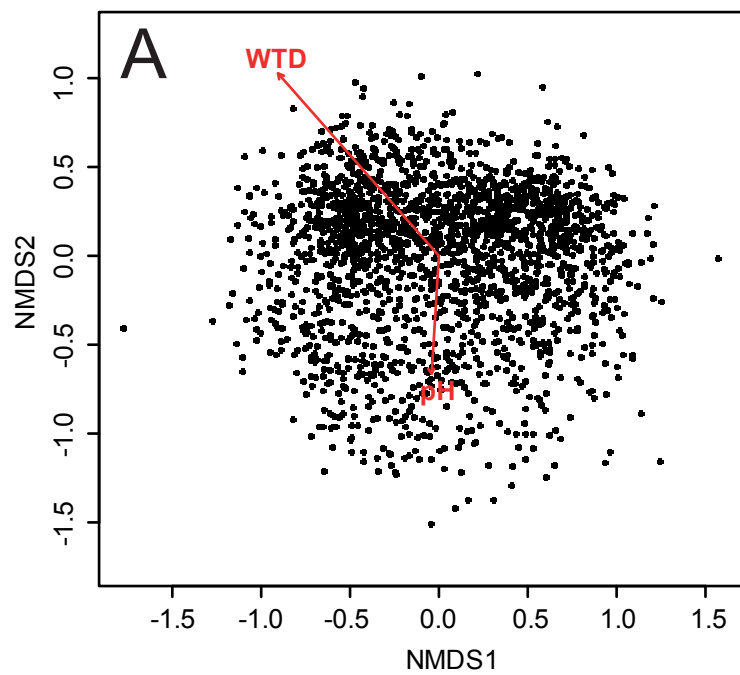
Sample number (ordered by water table depth, dry to wet)



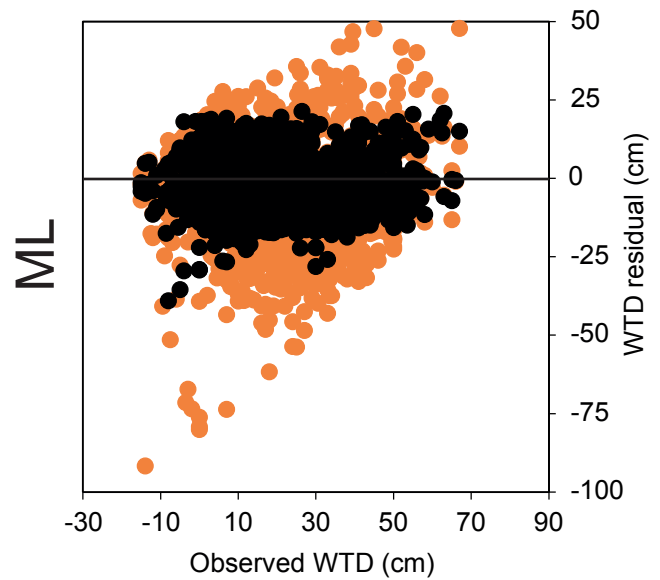
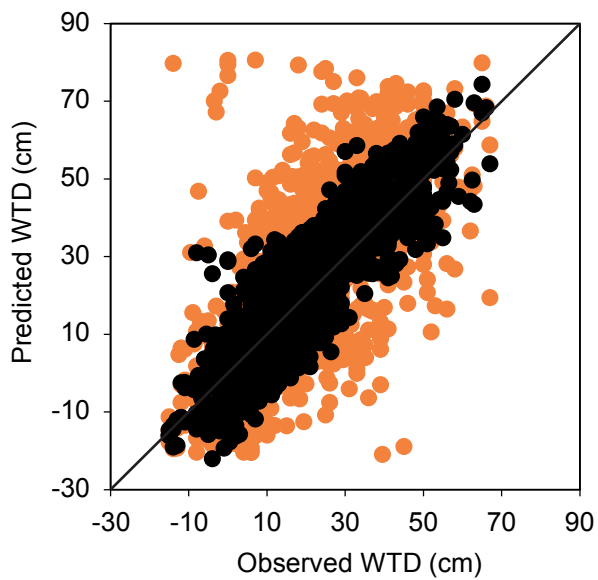
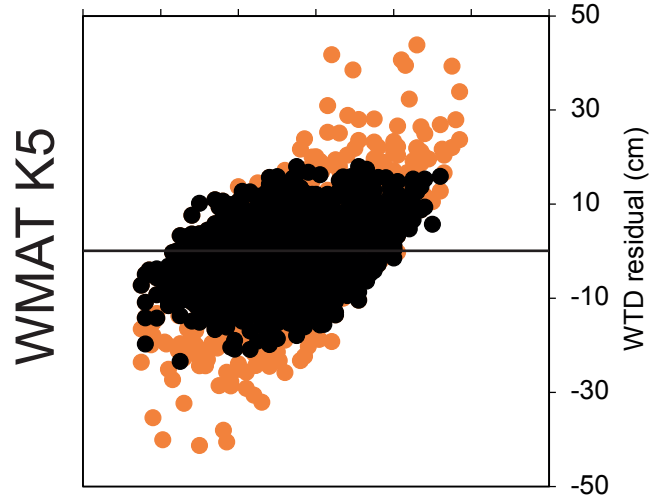
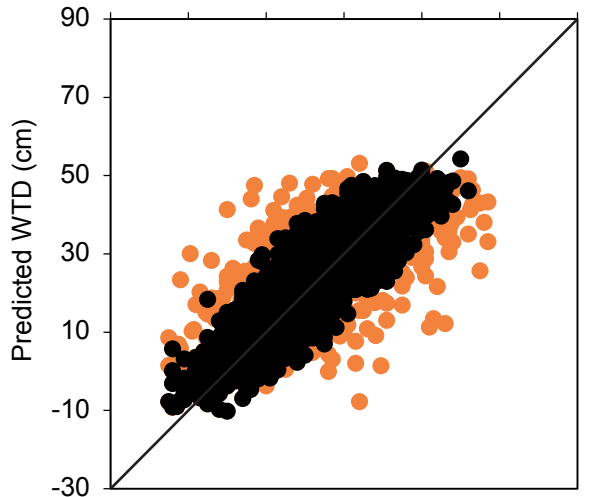
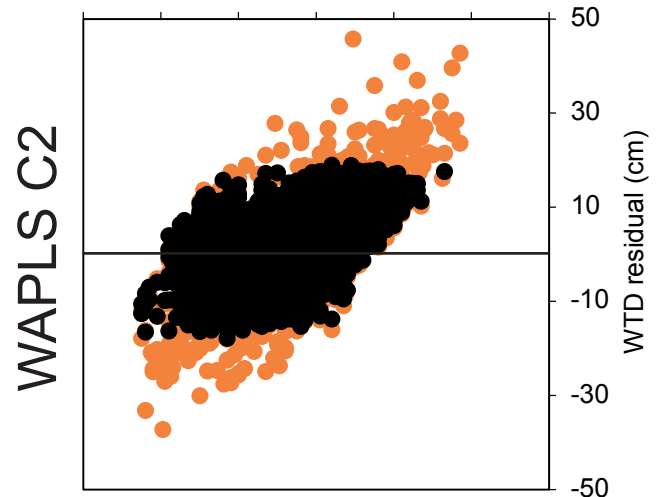
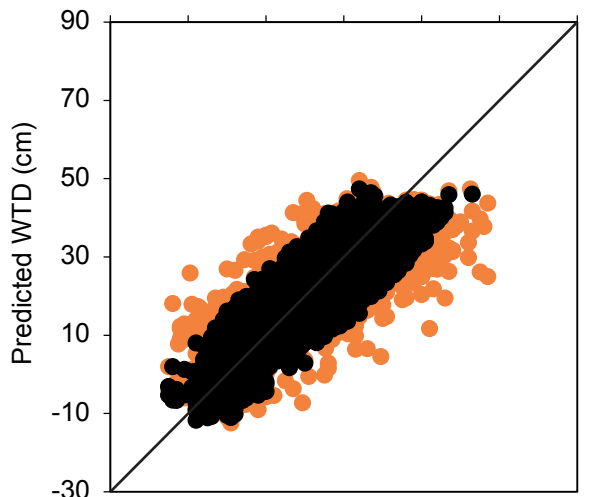
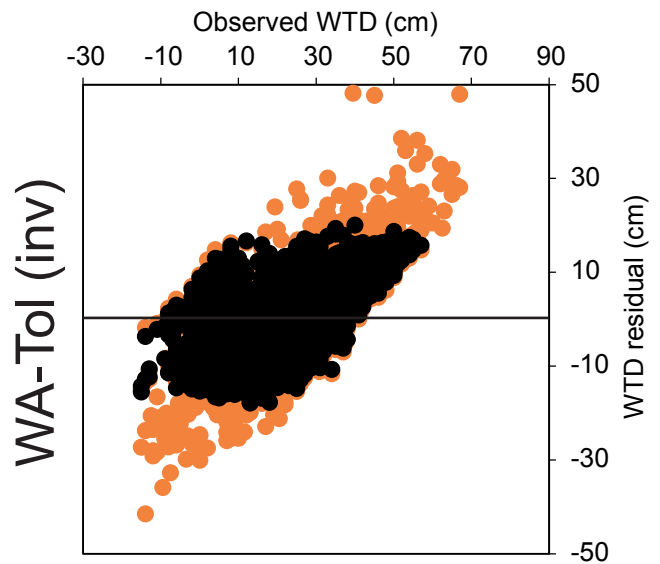
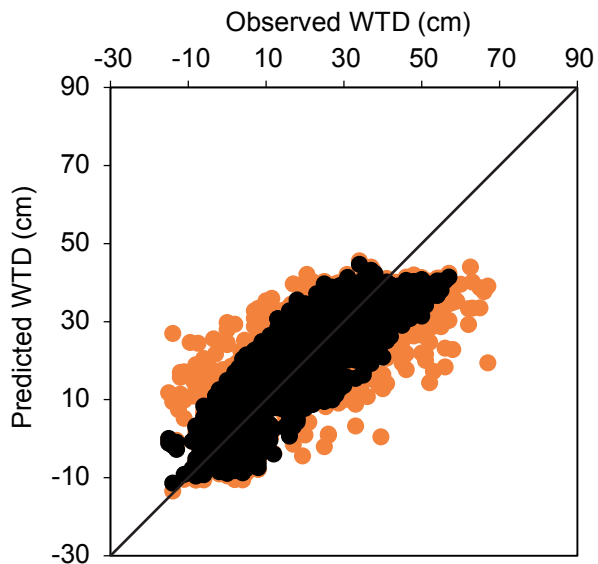
- Diffugia oviformis* type
- Diffugia globulosa* type
- Arcella vulgaris* type
- Diffugia bacilliarium* type
- Planocarina carinata* type
- Diffugia lucida* type
- Amphitrema wrightianum* type
- Diffugia rubescens*
- Diffugia urceolata* type
- Arcella hemispherica* type
- Arcella gibbosa* type
- Diffugia oblonga* type
- Diffugia leidy*
- Diffugia acuminata* type
- Diffugia pristis* type
- Planocarina marginata* type
- Pseudodiffugia fulva* type
- Arcella discoides* type
- Placocista spinosa*
- Quadrulella symmetrica*
- Centropyxis platystoma* type
- Tracheléglypha dentata*
- Archerella flavum*
- Heleopera sphagni* type
- Diffugia pulex*
- Centropyxis aculeata* type
- Phryganella acropodia* type
- Physochila griseola* type
- Gibbocarina tubulosa* type
- Hyalosphenia papilio*
- Podaungiella wailesi* type
- Argynnia dentistoma* type
- Heleopera petricola* type
- Hyalosphenia elegans*
- Podaungiella lageniformis* type
- Sphenoderia lenta*
- Euglypha strigosa* type
- Nebela barbata*
- Euglypha ciliata* type
- Pseudodiffugia fascicularis* type
- Heleopera rosea*
- Nebela collaris* type
- Centropyxis cassis* type
- Cryptodiffugia sacculus* type
- Nebela minor*
- Nebela penardiana* type
- Nebela flabellulum*
- Nebela tincta* type
- Euglypha tuberculata* type
- Euglypha rotunda* type
- Arcella catinus* type
- Alabasta militaris* type
- Arcella artocrea* type
- Heleopera sylvatica*
- Cyclopyxis arcelloides* type
- Hyalosphenia subflava*
- Corythion - Trinema* type
- Hyalosphenia minuta*
- Centropyxis ecoris* type
- Assulina muscorum* type
- Cryptodiffugia oviformis* type
- Assulina seminulum* type
- Bullinularia indica*
- Trigonopyxis arcula* type

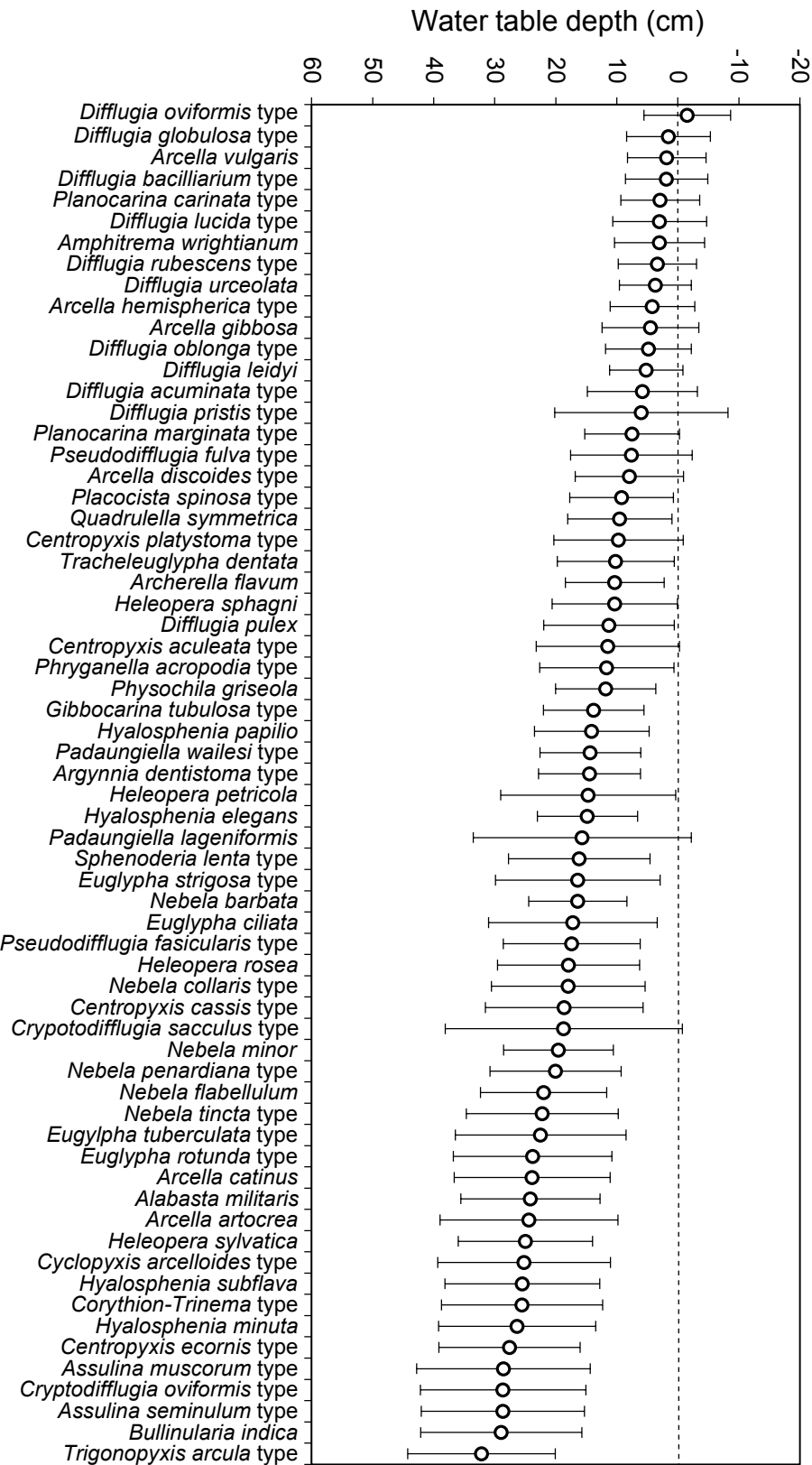
Water-table depth (cm)
(Scale range -20 to 60 cm)

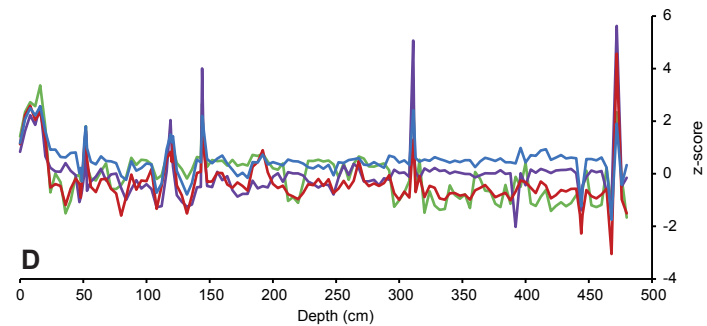
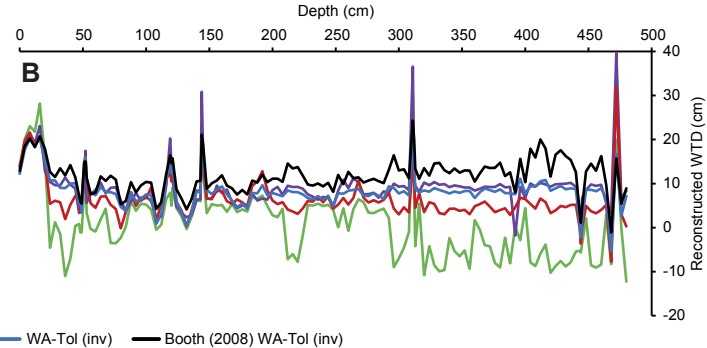
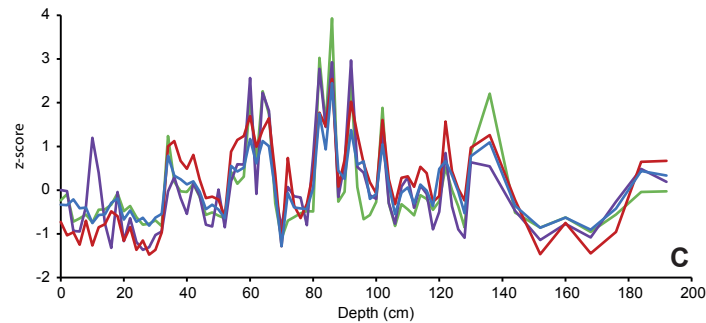
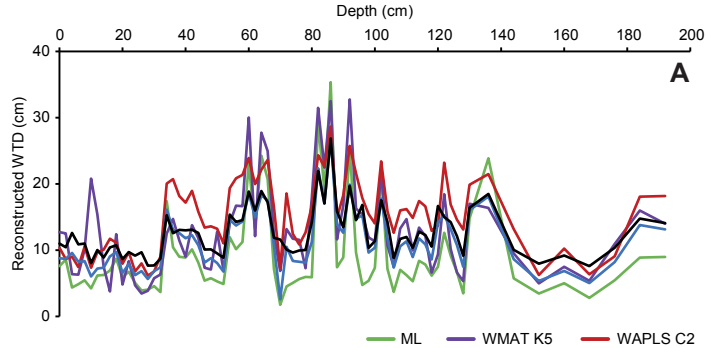
All taxa proportions are % values

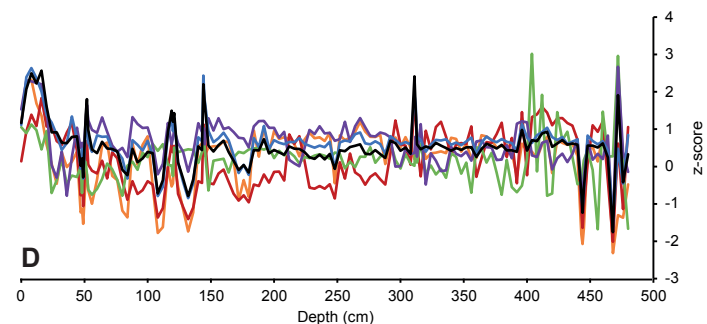
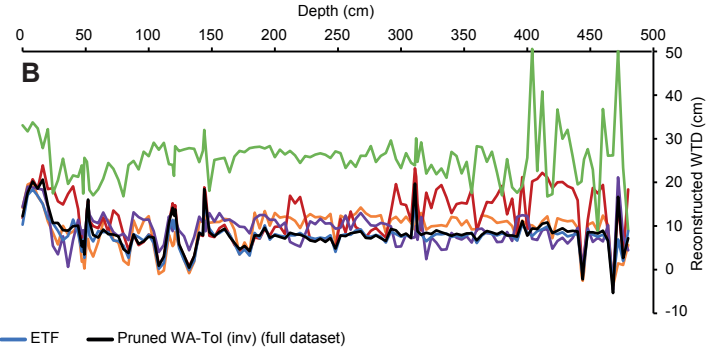
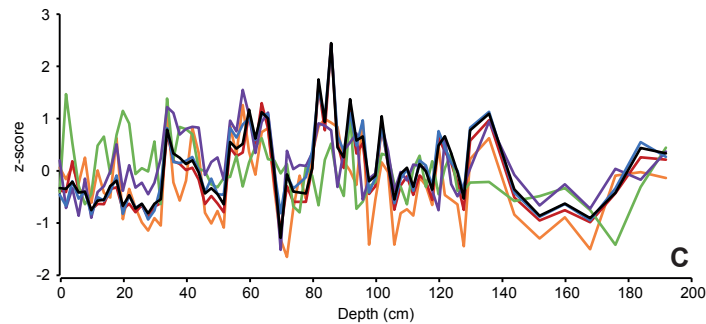
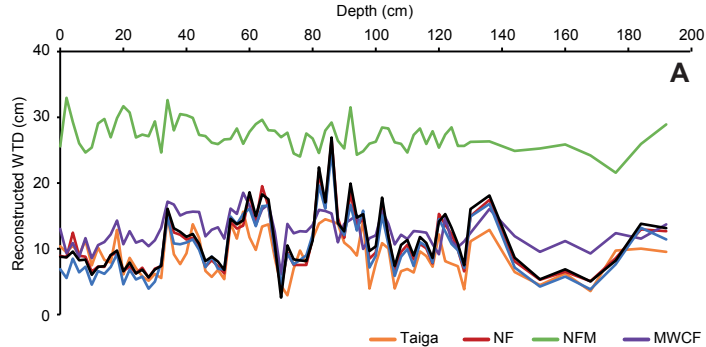


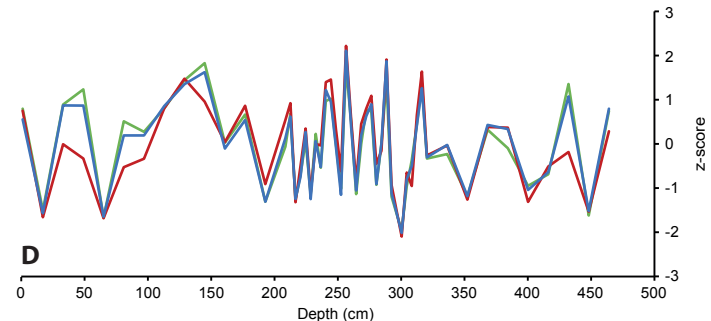
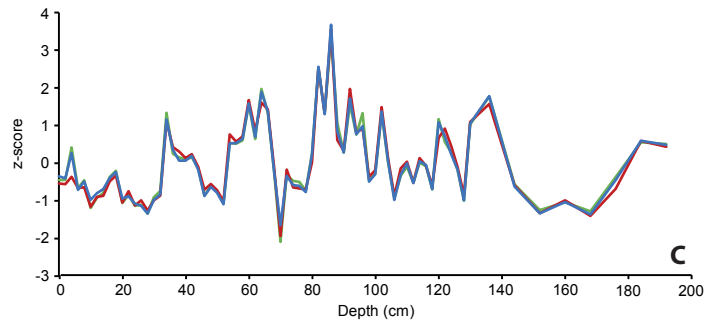
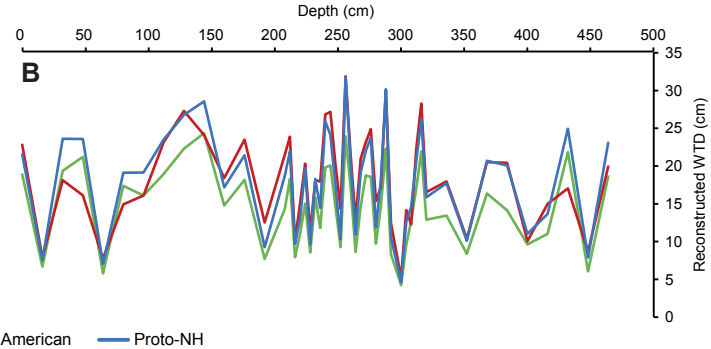
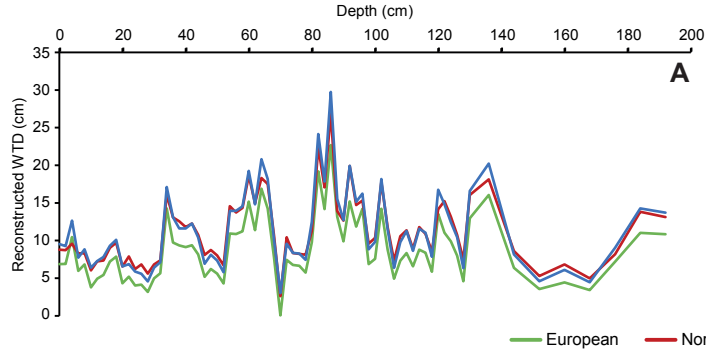
- Northern forests
- △ Eastern temperate forest
- + Northwestern forested mountains
- × North American desert
- ◇ Marine west coast forest
- ▽ Taiga
- Hudson plain
- * Tundra











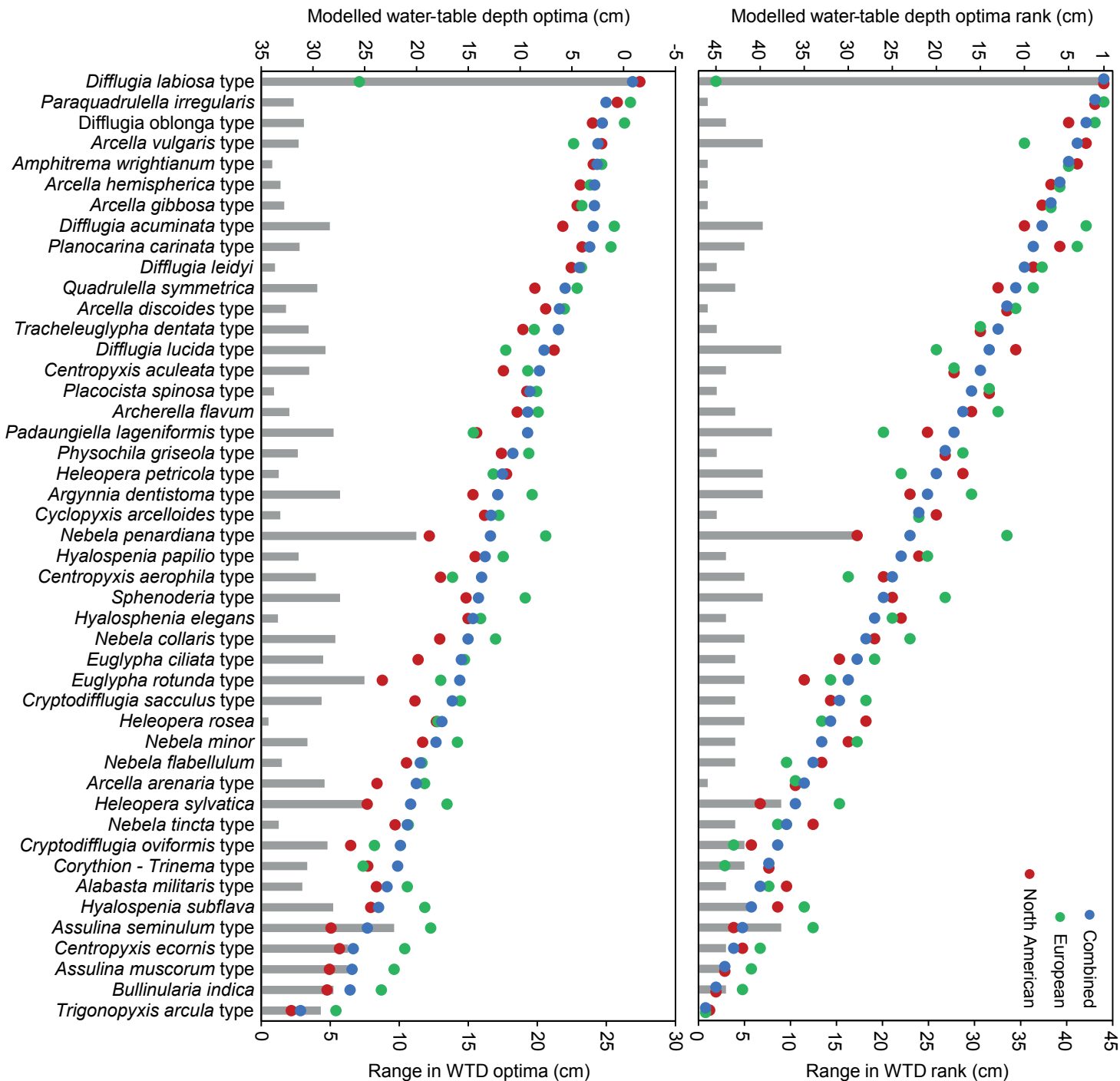


Table 1: Site details and meta-data. Data ordered by year of publication/surname and listed alphabetically by site name. For Warner and Charman (1994), sample codes could not be confidently linked to specific sites, so only the total number of samples in the dataset is shown.

Reference	State/Province, Country	Site name	Lat (°)	Long (°)	Number of samples
Warner (1987)	Ontario, Canada	Chesney	43.226	-80.644	4
Warner (1987)	Ontario, Canada	Ellice Huckleberry Marsh	43.481	-80.949	2
Warner (1987)	Ontario, Canada	Kossuth	43.449	-80.359	3
Warner (1987)	Ontario, Canada	Sifton	42.970	-81.323	6
Warner (1987)	Ontario, Canada	Summit Muskeg Preserve	43.231	-80.052	7
Charman and Warner (1992)	Ontario, Canada	Wally Creek	49.076	-80.537	108
Warner and Charman (1994)	Minnesota, USA	Beckman Lake	45.421	-93.186	49
Warner and Charman (1994)	Ontario, Canada	Buriss	48.666	-93.632	
Warner and Charman (1994)	Minnesota, USA	Cedar Lake	45.412	-93.198	
Warner and Charman (1994)	Ontario, Canada	Emo	48.702	-93.825	
Warner and Charman (1994)	Ontario, Canada	Fort Frances Airport	48.545	-93.398	
Warner and Charman (1994)	Ontario, Canada	Kehl Lake	48.579	-93.576	
Warner and Charman (1994)	Ontario, Canada	Pinewood	48.754	-94.290	
Warner and Charman (1994)	Ontario, Canada	Rainy River	48.758	-94.533	
Warner and Charman (1994)	Ontario, Canada	Stratton	48.680	-94.124	
Booth (2001), Booth (2002)	Michigan, USA	Grand Traverse Bay	47.166	-88.255	40
Booth (2001), Booth (2002)	Michigan, USA	Tahquamenon	46.475	-84.995	55
Booth (2002), Booth (2008)	Michigan, USA	Adam's Trail	46.547	-86.06	21
Booth (2002)	Michigan, USA	Au Train	46.548	-86.059	23
Booth (2002)	Michigan, USA	Independence	47.419	-88.01	29
Booth (2002), Booth (2008)	Michigan, USA	Minden	43.61	-82.836	43
Booth (2002), Booth (2008)	Michigan, USA	North Rhody	46.583	-86.073	24
Booth (2002)	Michigan, USA	Partridge	47.42	-88.008	22

Booth (2002), Booth (2008)	Michigan, USA	South Rhody	46.565	-86.075	32
Booth (2002)	Michigan, USA	Uncle Sam	47.419	-88.016	8
Booth (2002)	Michigan, USA	West Adam's Trail	46.553	-86.105	4
Booth and Zygmunt (2005)	Colorado, USA	Burro Bridge	37.846	-107.727	8
Booth and Zygmunt (2005)	New Mexico, USA	Chatanooga	36.961	-107.693	14
Booth and Zygmunt (2005)	Wyoming, USA	East Lily	44.954	-109.696	10
Booth and Zygmunt (2005)	Colorado, USA	Henderson A	39.367	-106.583	5
Booth and Zygmunt (2005)	Colorado, USA	Henderson B	39.354	-106.603	8
Booth and Zygmunt (2005)	Colorado, USA	Keystone	38.867	-107.04	9
Booth and Zygmunt (2005)	Wyoming, USA	Lilypad	44.164	-111.008	15
Booth and Zygmunt (2005)	Wyoming, USA	Little Moose	44.976	-109.757	12
Booth and Zygmunt (2005)	Idaho, USA	Lizard	44.156	-111.071	5
Booth and Zygmunt (2005)	Wyoming, USA	Robinson	44.167	-111.071	15
Booth and Zygmunt (2005)	Colorado, USA	Shafer	40.866	-106.605	9
Booth and Zygmunt (2005)	Colorado, USA	South Mineral	37.816	-107.723	8
Booth and Zygmunt (2005)	Colorado, USA	Splain's Gulch	38.834	-107.076	7
Booth and Zygmunt (2005)	Colorado, USA	Wager Gulch	37.878	-107.369	9
Booth and Zygmunt (2005)	Idaho, USA	West Robinson	44.167	-111.075	5
Payne et al. (2006)	Alaska, USA	Bicentennial Park	61.160	-149.743	28
Payne et al. (2006)	Alaska, USA	Clam Gulch	60.239	-151.375	3
Payne et al. (2006)	Alaska, USA	Houston	61.640	-149.863	9
Payne et al. (2006)	Alaska, USA	Jigsaw Lake	60.739	-150.490	18
Payne et al. (2006)	Alaska, USA	Kachemak	59.792	-151.169	8
Payne et al. (2006)	Alaska, USA	Moose Pass	60.509	-149.442	8
Payne et al. (2006)	Alaska, USA	Sheep Creek	62.003	-150.055	9
Payne et al. (2006)	Alaska, USA	Sterling	60.528	-150.518	8
Booth (2008)	Michigan, USA	Big Red Pine	46.253	-86.623	10
Booth (2008)	New York, USA	Bloomingtondale	44.383	-74.139	19

Booth (2008)	Wisconsin, USA	Crystal	46.007	-89.605	13
Booth (2008)	Minnesota, USA	Ely	47.446	-92.436	9
Booth (2008)	Wisconsin, USA	Fallston	45.995	-89.613	15
Booth (2008)	Michigan, USA	Grimes	46.276	-86.65	10
Booth (2008)	Michigan, USA	Herron	45.102	-83.639	10
Booth (2008)	Michigan, USA	Hole-in-bog	47.3	-94.249	14
Booth (2008)	Wisconsin, USA	Hornet	46.077	-92.12	15
Booth (2008)	Michigan, USA	Island Camp	46.272	-86.647	11
Booth (2008)	Michigan, USA	Kentucky Trail	46.247	-86.601	10
Booth (2008)	Maine, USA	Orono	44.871	-68.727	18
Booth (2008)	Vermont, USA	Peacham	44.292	-72.873	12
Booth (2008)	Michigan, USA	Small Red Pine	46.238	-86.617	5
Booth (2008)	Wisconsin, USA	Small Sarracenia	46.093	-92.115	10
Booth (2008)	New York, USA	Spring Pond	44.368	-74.499	26
Booth (2008)	Wisconsin, USA	Spruce	46.095	-92.112	8
Booth (2008)	Minnesota, USA	Toivola A	46.927	-92.795	13
Booth (2008)	Minnesota, USA	Toivola B	46.986	-92.888	6
Booth (2008)	Wisconsin, USA	Trout Lake	46.004	-89.594	68
Booth (2008)	Michigan, USA	Upper Twin	46.276	-86.647	10
Booth et al. (2008)	North Carolina, USA	Catfish Pocosin	34.919	-77.088	35
Markel et al. (2010)	Alaska, USA	Brown's Lake	60.471	-150.728	38
Markel et al. (2010)	Alaska, USA	Canaday	64.519	-146.911	8
Markel et al. (2010)	Alaska, USA	Caswell	62.004	-150.060	5
Markel et al. (2010)	Alaska, USA	Funny River	60.415	-150.901	8
Markel et al. (2010)	Alaska, USA	Gate Creek	62.333	-150.545	8
Markel et al. (2010)	Alaska, USA	Jake Lake	62.430	-150.704	7
Markel et al. (2010)	Alaska, USA	Gas Field	60.445	-151.246	24
Markel et al. (2010)	Alaska, USA	Marathon B	60.603	-151.211	5

Markel et al. (2010)	Alaska, USA	No Name	60.640	-151.08	5
Markel et al. (2010)	Alaska, USA	Parks Highway	63.081	-149.527	7
Markel et al. (2010)	Alaska, USA	Richardson	62.604	-145.448	3
Markel et al. (2010)	Alaska, USA	Teardrop Lake	60.472	-150.700	6
Sullivan and Booth (2011)	Pennsylvania, USA	Tannersville	41.037	-75.266	47
Sullivan and Booth (2011)	Pennsylvania, USA	Titus	41.952	-79.759	20
Amesbury et al. (2013)	Newfoundland, Canada	Burnt Village	51.126	-55.927	25
Amesbury et al. (2013)	Nova Scotia, Canada	Colin	45.108	-63.895	27
Amesbury et al. (2013), Charman and Warner (1997)	Newfoundland, Canada	Crooked	49.139	-56.111	14
Amesbury et al. (2013)	Quebec, Canada	Kegaska	50.211	-61.25	4
Amesbury et al. (2013), Lamarre et al. (2013)	Quebec, Canada	Lebel	49.123	-68.292	19
Amesbury et al. (2013), Lamarre et al. (2013)	Quebec, Canada	Manic	49.123	-68.292	30
Amesbury et al. (2013)	Newfoundland, Canada	Nordan's Pond	49.161	-53.598	20
Amesbury et al. (2013), Charman and Warner (1997)	Newfoundland, Canada	Ocean Pond	47.427	-53.438	9
Amesbury et al. (2013)	Nova Scotia, Canada	Petite	45.144	-63.937	16
Amesbury et al. (2013), Lamarre et al. (2013)	Quebec, Canada	Plaine	50.27	-63.54	21
Amesbury et al. (2013)	Maine, USA	Saco	43.553	-70.471	26
Amesbury et al. (2013), Charman and Warner (1997)	Newfoundland, Canada	Sam's River	46.731	-53.519	6
Amesbury et al. (2013)	Quebec, Canada	Sept Isles	50.202	-66.601	6
Amesbury et al. (2013)	Maine, USA	Sidney	44.388	-69.788	24
Amesbury et al. (2013), Charman and Warner (1997)	Newfoundland, Canada	Stephenville	48.55	-58.434	6
Amesbury et al. (2013)	Quebec, Canada	Tourbiere de l'Aeroport	50.275	-63.614	7
Amesbury et al. (2013), Charman and Warner (1997)	Newfoundland, Canada	Witless Bay	47.337	-53.017	4
Lamarre et al. (2013)	Quebec, Canada	Abeille	54.115	-73.327	6
Lamarre et al. (2013)	Quebec, Canada	Baie-M	49.093	-68.243	11
Lamarre et al. (2013)	Quebec, Canada	Baie Commeau	49.097	-68.244	7
Lamarre et al. (2013)	Quebec, Canada	Frontenac	45.966	-71.139	10
Lamarre et al. (2013)	Quebec, Canada	Kuujuarapik	55.226	-77.696	10

Lamarre et al. (2013)	Quebec, Canada	La Grande Bog	53.65	-77.726	10
Lamarre et al. (2013)	Quebec, Canada	La Grande Fen	53.677	-78.216	10
Lamarre et al. (2013)	Quebec, Canada	Lebel-G	49.101	-68.219	10
Lamarre et al. (2013)	Quebec, Canada	Matagami 1	49.752	-77.657	6
Lamarre et al. (2013)	Quebec, Canada	Matagami 2	49.685	-77.732	10
Lamarre et al. (2013)	Quebec, Canada	Morts	50.264	-63.669	17
Lamarre et al. (2013)	Quebec, Canada	Pylone	53.797	-73.327	3
Lamarre et al. (2013)	Quebec, Canada	Roma	50.298	-63.693	25
Lamarre et al. (2013)	Quebec, Canada	Val d'Or	48.187	-77.595	10
Lamarre et al. (2013)	Quebec, Canada	Verendrye	47.303	-76.855	4
Roe et al. (2017)	Ontario, Canada	Alfred	45.494	-74.805	47
Roe et al. (2017)	Ontario, Canada	Mirabel	45.685	-74.045	40
Roe et al. (2017)	Quebec, Canada	Mer Bleue	45.402	-75.486	58
Clifford (unpublished)	British Columbia, Canada	Burns	49.123	-122.970	12
Clifford (unpublished)	British Columbia, Canada	Eagle Creek	58.284	-134.521	12
Clifford (unpublished)	British Columbia, Canada	Fish Creek	58.336	-134.554	12
Clifford (unpublished)	British Columbia, Canada	Point Bridget	58.647	-134.934	12
Clifford (unpublished)	British Columbia, Canada	Point Lena	58.386	-134.746	12
Clifford (unpublished)	British Columbia, Canada	Surrey	49.204	-122.747	12
Finkelstein/Bunbury (unpublished)	Ontario, Canada	Attawapiskat River 1	52.845	-83.927	16
Finkelstein/Bunbury (unpublished)	Ontario, Canada	Attawapiskat River 2	52.720	-83.940	11
Finkelstein/Bunbury (unpublished)	Ontario, Canada	Attawapiskat River 3	52.712	-84.174	5
Finkelstein/Bunbury (unpublished)	Ontario, Canada	Sutton River 1	55.752	-84.525	2
Finkelstein/Bunbury (unpublished)	Ontario, Canada	Sutton River 2	54.676	-84.599	5
Finkelstein/Bunbury (unpublished)	Ontario, Canada	Sutton River 3	54.610	-84.609	5
Finkelstein/Bunbury (unpublished)	Ontario, Canada	Sutton River 4	54.599	-84.640	3
Swindles (unpublished)	Alaska, USA	Toolik	68.624	-149.580	7
Talbot (unpublished)	Ontario, Canada	Folly	45.272	-75.466	1

Talbot (unpublished)	Quebec, Canada	Mont St. Bruno	45.335	-73.215	2
Talbot (unpublished)	Northwest Territories, Canada	Scotty Creek	61.307	-121.298	21
				TOTAL:	1956

Table 2: Full taxonomy applied in this study.

#	Abbreviation	Full name	Also includes
1	ALA MIL	Alabasta (Nebela) militaris type	
2	AMP WRI	Amphitrema wrightianum type	Amphitrema stenostoma
3	ARC ART	Arcella artocrea	
4	ARC CAT	Arcella catinus type	Arcella arenaria type
5	ARC DIS	Arcella discoides type	
6	ARC GIB	Arcella gibbosa type	
7	ARC HEM	Arcella hemispherica type	Arcella rotundata
8	ARC VUL	Arcella vulgaris type	Arcella crenulata
9	ARC FLA	Archerella flavum	
10	ARG DEN	Argynnia dentistoma type	Nebela dentistoma Nebela vitraea type
11	ASS MUS	Assulina muscorum	
12	ASS SEM	Assulina seminulum type	Assulina scandinavica
13	BUL IND	Bullinularia indica	
14	CEN ACU	Centropyxis aculeata type	
15	CEN CAS	Centropyxis cassis type	Centropyxis aerophila type Centropyxis constricta type
16	CEN PLA	Centropyxis platystoma type	
17	CEN ECO	Centropyxis ecornis type	Centropyxis delicatula type Centropyxis laevigata type
18	CON PON	Conicocassis pontigulasiformis	
19	COR TRI	Corythion - Trinema type	Corythion dubium

			Corythion complanatum Trinema enchelys Trinema lineare Trinema sp.
20	CRY OVI	Cryptodiffugia oviformis type	
21	CRY SAC	Cryptodiffugia sacculus	
22	CYC ARC	Cyclopyxis arcelloides type	Cyclopyxis kahli type
23	CYP AMP	Cyphoderia ampulla type	Cyphoderia calceolus
24	DIF ACU	Diffugia acuminata type	Diffugia bacilliarum type
25	DIF BAC	Diffugia bacillifera type	
26	DIF GLO	Diffugia globulosa type	
27	DIF LEI	Diffugia leidy	
28	DIF LUC	Diffugia lucida type	
29	DIF OBL	Diffugia oblonga type	Diffugia lanceolata
30	DIF OVI	Diffugia oviformis type	Diffugia lithophila type Netzelia (Diffugia) tuberculata type
31	DIF PRI	Diffugia pristis type	
32	DIF PUL	Diffugia pulex type	
33	DIF RUB	Diffugia rubescens type	
34	DIF URC	Diffugia urceolata type	
35	EUG CIL	Euglypha ciliata type	Euglypha compressa Euglypha cristata
36	EUG ROT	Euglypha rotunda type	
37	EUG STR	Euglypha strigosa type	
38	EUG TUB	Euglypha tuberculata type	
39	GIB TUB	Gibbocarina (Nebela) tubulosa type	
40	HEL ROS	Heleopera rosea	
41	HEL PET	Heleopera petricola	
42	HEL SPH	Heleopera sphagni	
43	HEL SYL	Heleopera sylvatica	

44	HYA ELE	Hyalosphenia elegans	
45	HYA MIN	Hyalosphenia minuta	
46	HYA PAP	Hyalosphenia papilio	
47	HYA SUB	Hyalosphenia subflava	
48	LES EPI	Lesquereusia epistomum	
49	LES MOD	Lesquereusia modesta type	Lesquereusia spiralis type
50	NEB BAR	Nebela barbata	
51	NEB COL	Nebela collaris type	Hyalosphenia ovalis
52	NEB FLA	Nebela flabellulum	
53	NEB MIN	Nebela minor	
54	NEB PEN	Nebela penardiana type	
55	NEB TIN	Nebela tincta type	Nebela bohémica Nebela parvula
56	PAD LAG	Padaungiella (Nebela) lageniformis	
57	PAD WAI	Padaungiella (Nebela) waillesi	
58	PAR IRR	Paraquadrula irregularis	Paraquadrula sp.
59	PHR ACR	Phryganella acropodia type	
60	PHY GRI	Physochila griseola type	(Nebela griseola type)
61	PLA CAL	Plagiopyxis callida type	
62	PLA SPI	Placocista spinosa type	Placocista lens
63	PLA CAR	Planocarina (Nebela) carinata type	Gibbocarina (Nebela) galeata type
64	PLA MAR	Planocarina (Nebela) marginata type	
65	PSE FUL	Pseudodifflugia fulva type	
66	PSE FAS	Pseudodifflugia fascicularis type	
67	PYXI	Pyxidicula type	Pyxidicula patens Pyxidicula sp.
68	QUA SYM	Quadrulella symmetrica	
69	SPH LEN	Sphenoderia lenta	
70	TRA DEN	Tracheleuglypha dentata	

71	TRI ARC	Trigonopyxis arcula type	Trigonopyxis minuta type
72	WAI EBO	Waileseila eboracensis	

Table 3: Numbers of sites, samples and taxa in different EPA eco-regions, along with information on water table depth (WTD) values for all samples within each region and basic performance statistics for eco-region transfer functions derived from the pruned WA-Tol (inv) model dataset (n = 1696). Comparable data for all samples is shown in top row for reference. SD = standard deviation. SWDI = Shannon Wiener diversity index. Dashed lines indicate where no performance statistics are available as models were not run for all eco-regions due to low sample sizes.

Ecoregion	Number of samples	Number of sites	Number of taxa	Mean WTD \pm 1 SD (cm)	WTD range (min - max) (cm)	SWDI \pm 1 SD	RMSEP _{LoO}	R ²	Maximum bias	Average bias
ALL SAMPLES	1696	126	64	18.3 \pm 14.1	72 (-15 - 57)	1.95 \pm 0.44	7.42	0.72	13.87	0.02
Tundra	7	1	25	11.7 \pm 10	29 (1 - 30)	1.96 \pm 0.24	-	-	-	-
Taiga	64	6	56	12 \pm 10.1	49 (-3 - 46)	2.01 \pm 0.49	8.06	0.36	32.52	0.71
Hudson plain	32	7	44	15 \pm 14.2	47 (-4 - 43)	1.90 \pm 0.43	-	-	-	-
Northern forests	915	55	62	18.2 \pm 14.2	71 (-15 - 56)	2.01 \pm 0.41	6.90	0.76	15.53	0.46
Northwestern forested mountains	130	16	42	18.4 \pm 15.2	55 (-5 - 50)	1.70 \pm 0.55	6.87	0.80	13.89	0.29
Marine west coast forest	191	22	59	18.1 \pm 13.7	69 (-15 - 54)	1.91 \pm 0.36	8.30	0.63	18.37	0.19
Eastern temperate forests	346	18	62	20 \pm 13.8	65 (-8 - 57)	1.94 \pm 0.46	7.12	0.73	15.96	0.05
North American deserts	11	1	18	29.5 \pm 17	50 (0 - 50)	1.47 \pm 0.62	-	-	-	-

Table 4: Performance statistics for all transfer function models for water-table depth based on leave-one-out ($RMSEP_{LOO}$), leave-one-site-out ($RMSEP_{LOSO}$) and segment-wise ($RMSEP_{SW}$) cross validation methods. Results are in order of performance as assessed by $RMSEP_{LOO}$ of the pruned model run. Results for $RMSEP_{LOO}$ are given for both pre- and post-removal of samples with high residual values (see text for details; figures in parentheses show performance statistics after the removal of outlier samples). Results for $RMSEP_{LOSO}$ and $RMSEP_{SW}$ are only given for pruned models. Relative decreases in model performance are between $RMSEP_{LOO}$ of the pruned models to $RMSEP_{LOSO}$ and $RMSEP_{SW}$. SD is the standard deviation of all water-table measurements included in each model after the removal of outliers. Results are only shown for the best performing version of each model type. WA-Tol (inv) = weighted averaging with tolerance downweighting and inverse deshrinking; WAPLS C2 = second component of weighted averaging partial least squares; ML = maximum likelihood; WMAT K5 = weighted averaging modern analogue technique with five nearest neighbours.

Model type	$RMSEP_{LOO}$	R^2 (LOO)	Maximum bias (LOO)	Average bias (LOO)	$RMSEP_{LOSO}$	Relative decrease LOO - LOSO	$RMSEP_{SW}$	Relative decrease LOO - SW	Number of outlier samples removed	n for post-outlier removal model	SD
WMAT K5	9.38 (6.83)	0.64 (0.79)	22.97 (10.84)	-0.79 (-0.73)	8.21	0.201	7.07	0.034	161	1767	14.85
WA-Tol (inv)	10.20 (7.42)	0.57 (0.72)	28.48 (13.87)	0.03 (0.02)	7.70	0.037	8.06	0.086	197	1730	14.10
WAPLS C2	10.10 (7.53)	0.58 (0.71)	27.38 (14.38)	0.02 (0.02)	7.85	0.042	8.18	0.086	190	1737	14.11
ML	14.76 (8.60)	0.53 (0.77)	10.31 (6.95)	-3.00 (-1.18)	8.67	0.008	8.75	0.017	410	1517	15.72

Table 5: PalaeoSig p values for the significance of reconstructions against models based on randomly generated data for the pruned versions of four model types and five eco-region models, against two independent test sets. See Tables 3 and 4 for further statistics on all models.

Model	Framboise	Lac Le Caron
WA-Tol (inv)	0.013	0.987
WAPLS C2	0.015	0.984
WMAT K5	0.002	0.709
ML	0.057	0.287
Taiga	0.485	0.943
Northern forests	0.015	0.729
Northwestern forested mountains	0.782	0.997
Marine west coast forest	0.471	0.871
Eastern temperate forests	0.007	0.940

Supplementary figure captions

Figure S1: Summary results for the calculation of segment-wise RMSEP. Histograms show sampling distribution in 12 segments for the full dataset ($n = 1927$). Coloured lines show RMSEP for each individual segment for the four main model types under investigation.

Figure S2: Spatial autocorrelation diagrams for the four model types under investigation. Plots show effect on r^2 of deleting sites at random (open circles), from the geographical neighbourhood of the test site (filled circles labelled with corresponding distances) or that are most environmentally similar (crosses) during cross-validation. Note variable y-axis scales.

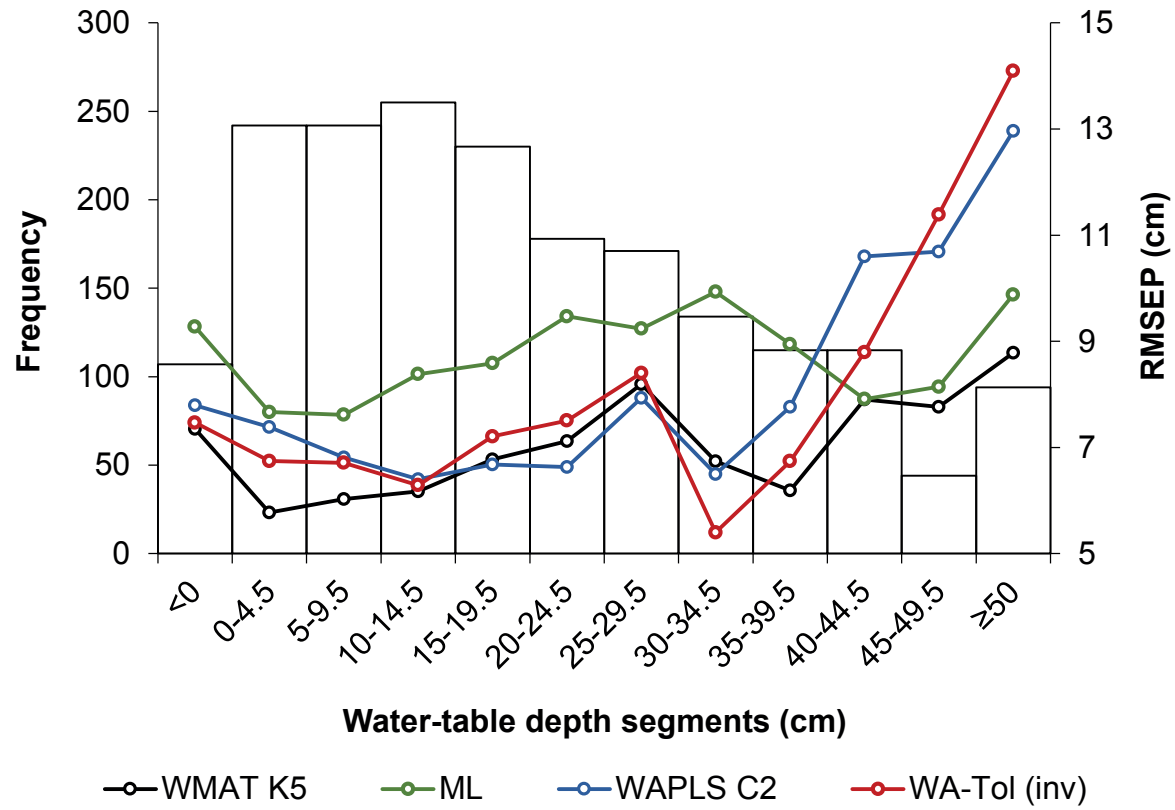
Figure S3: Water table depth reconstructions, with error, from two independent test sites for four different model types and the WA-Tol (inv) model of Booth (2008). Left-hand column is for Framboise bog, right-hand column is for Lac Le Caron peatland.

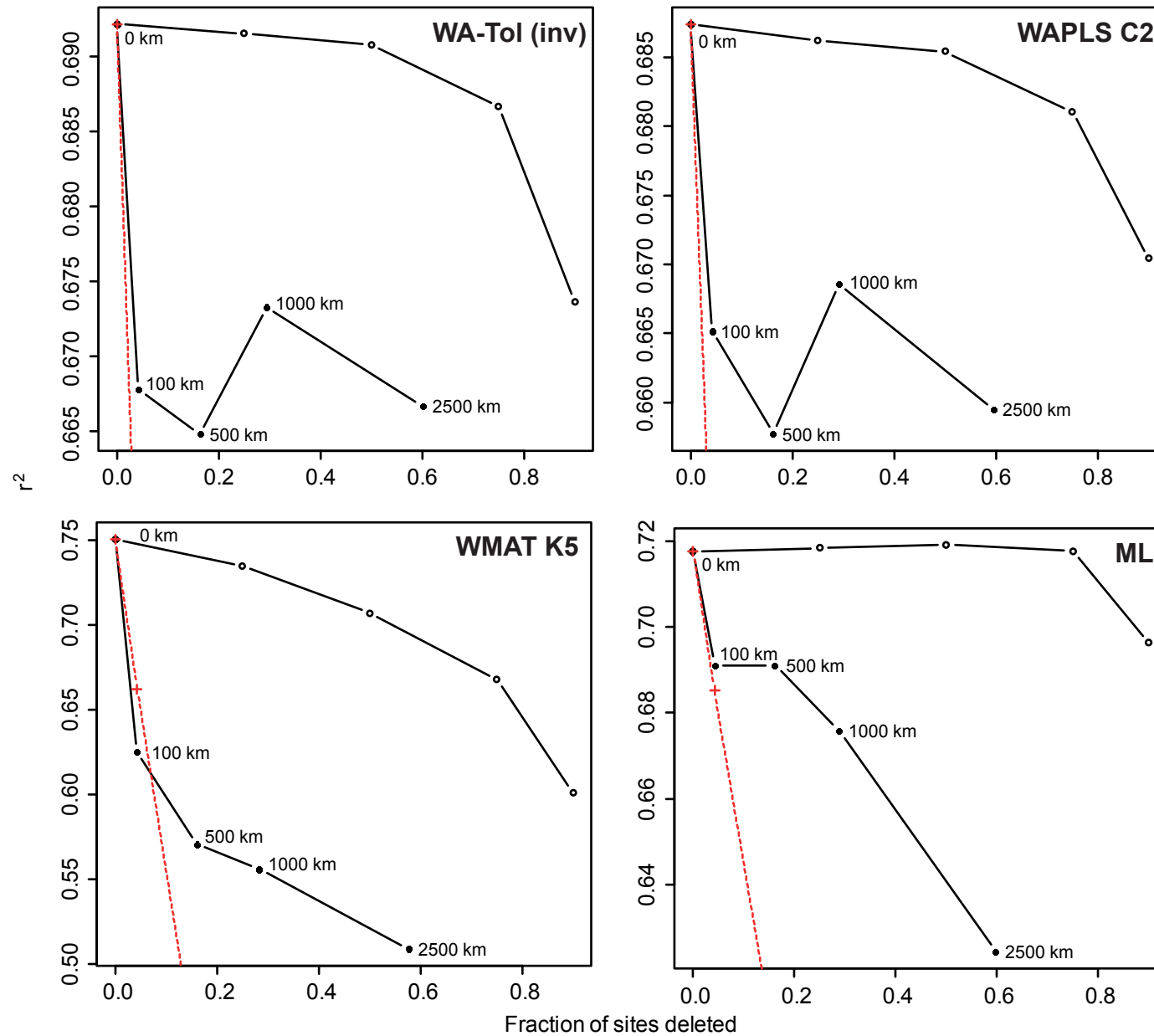
Figure S4: Water table depth reconstructions, with error, from two independent test sites for five different eco-region models, compared to the pruned WA-Tol (inv) model based on the full dataset. Left-hand column is for Framboise bog, right-hand column is for Lac Le Caron peatland. Model abbreviations in key: NF = Northern forests; NFM = Northwestern forested mountains; MWCF = Marine west coast forest; ETF = Eastern temperate forests.

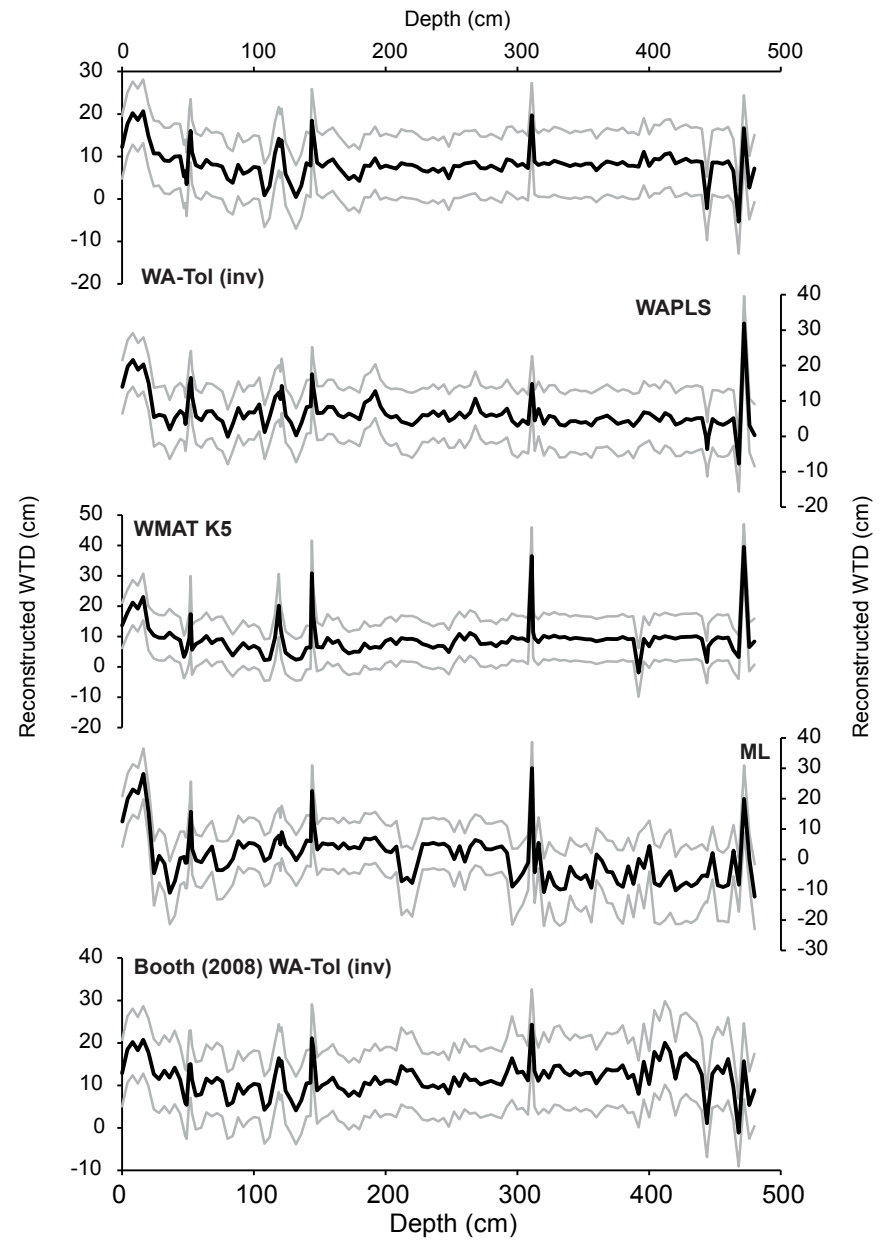
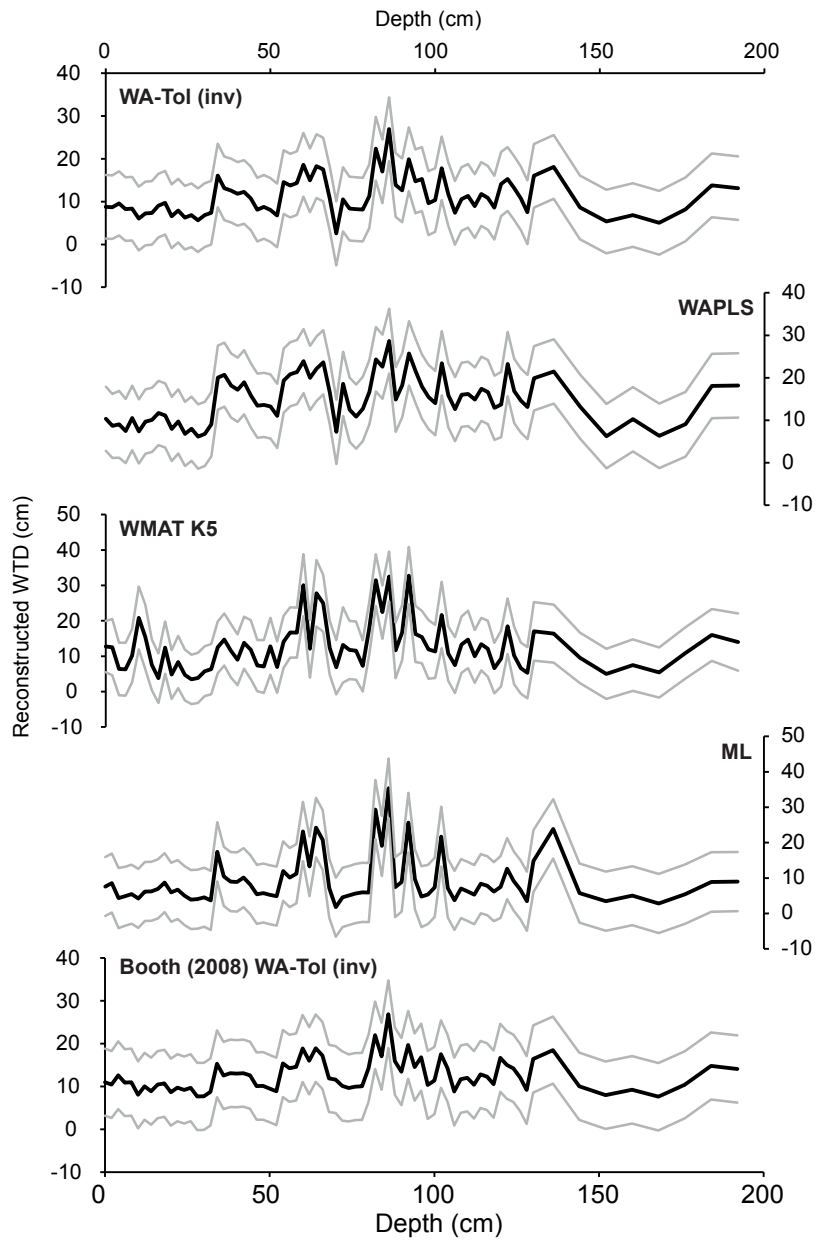
Figure S5: Distribution of all taxa (ordered alphabetically) across eight eco-regions. Eco-regions codes (x-axes): 1 = Tundra, 2 = Taiga, 3 = Hudson Plain, 4 = Northern forests, 5 = Northwestern forested mountains, 6 = Marine west coast forest, 7 = Eastern temperate forests, 8 = North American deserts. Y-axes show % abundance of the named taxon in all samples in which it occurs. Number of occurrences in 1884 samples shown in brackets after each taxon code. For taxa name abbreviations, see Table 2.

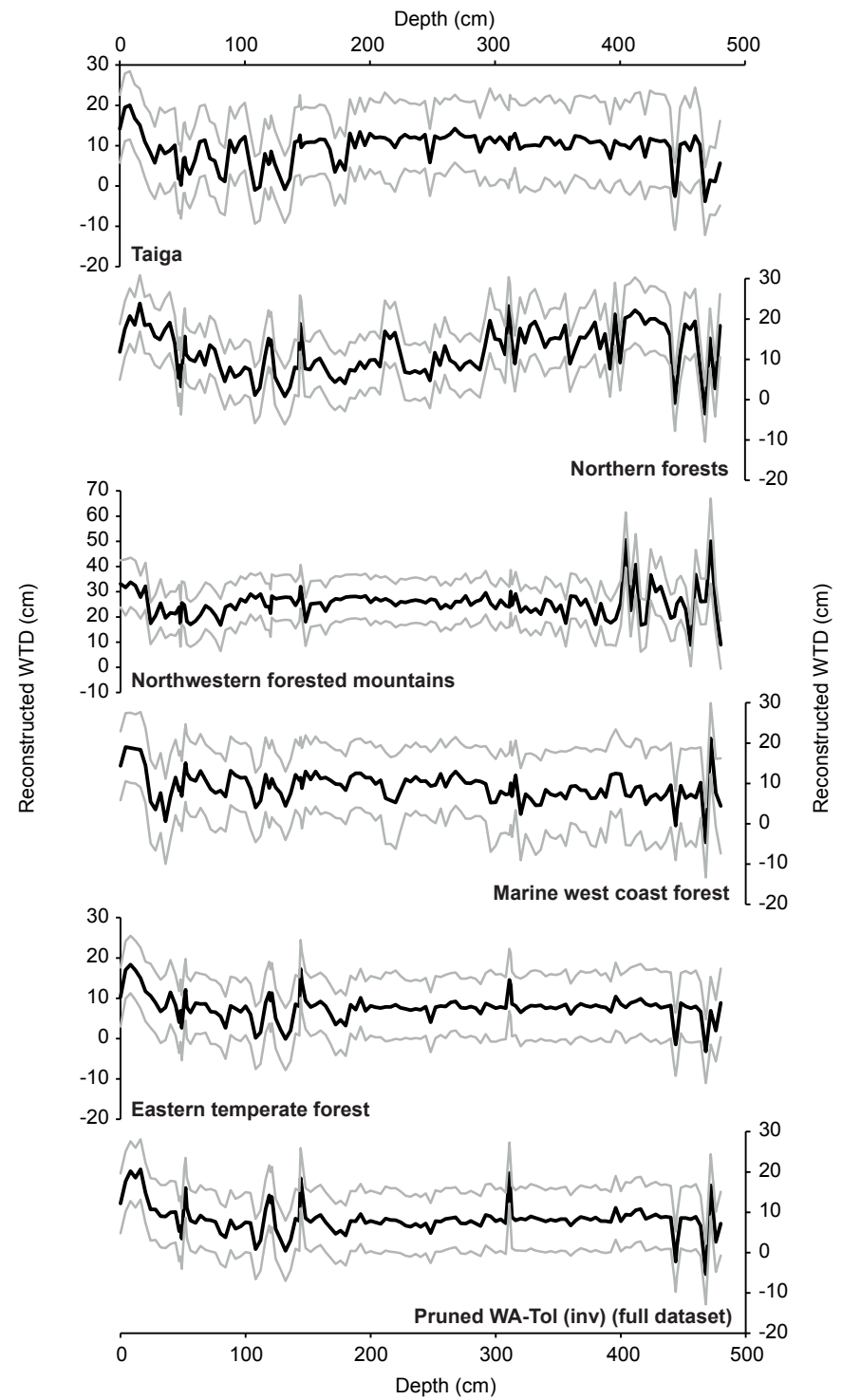
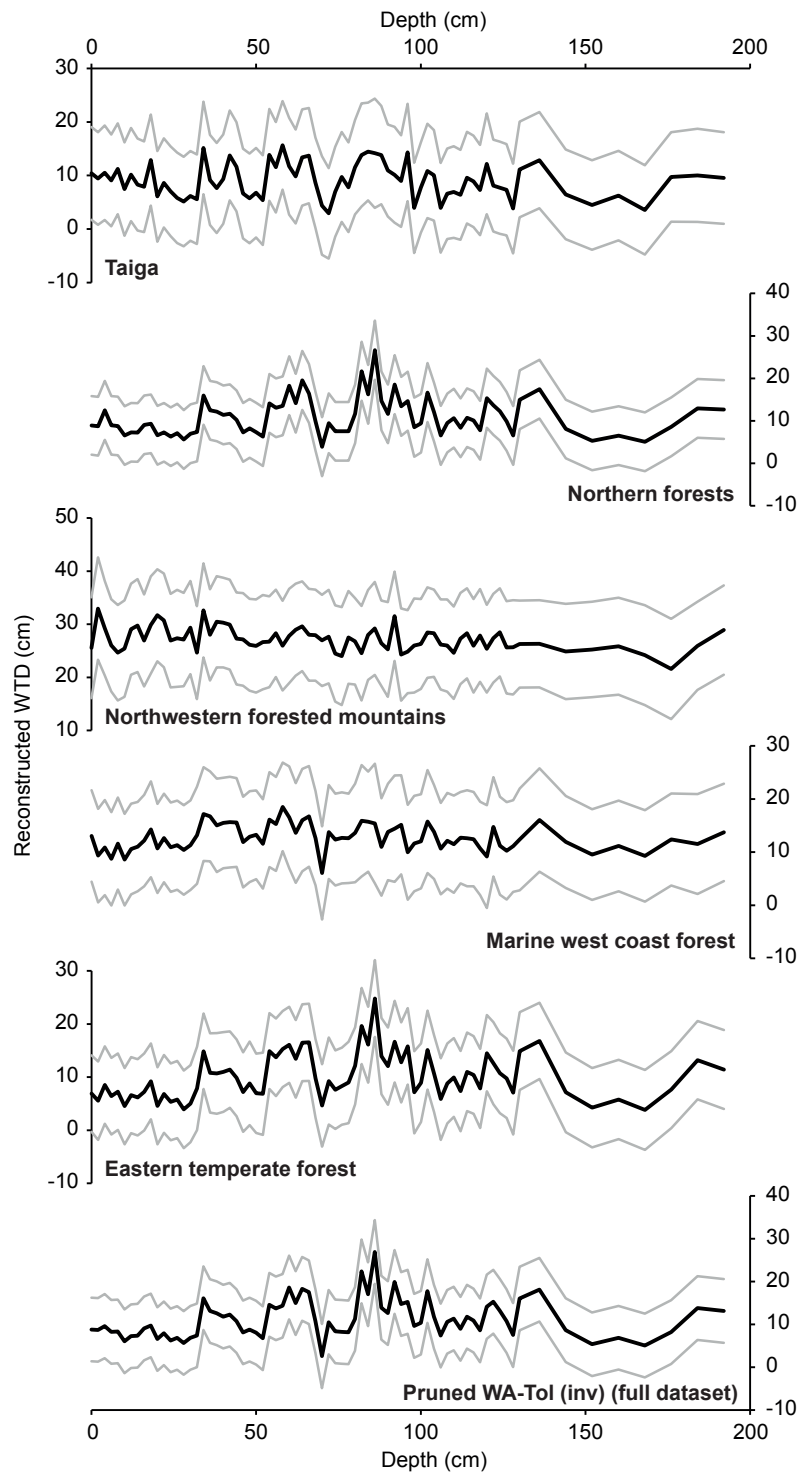
Figure S6: Comparison of occurrence (i.e. % presence in all samples; black bars), abundance (i.e. maximum % abundance in any one sample; grey bars) and presence in n eco-regions (red line) for all 64 taxa included in the full dataset.

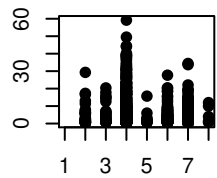
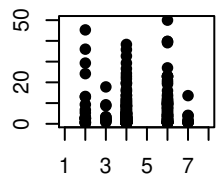
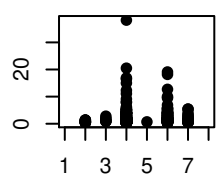
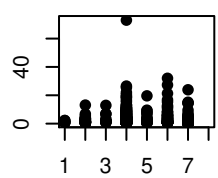
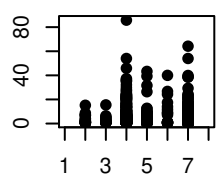
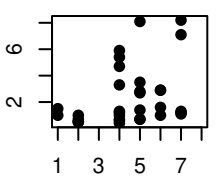
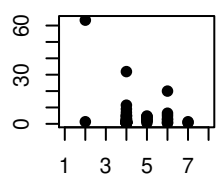
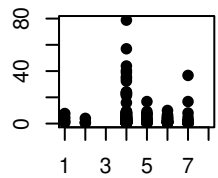
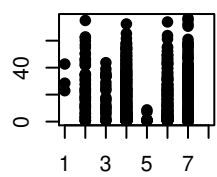
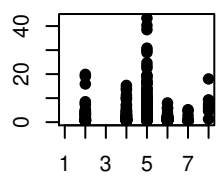
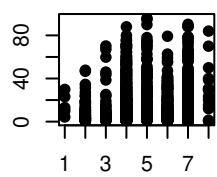
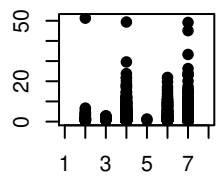
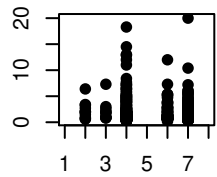
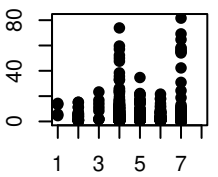
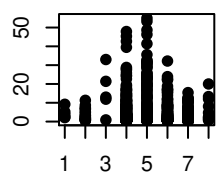
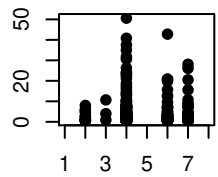
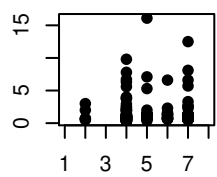
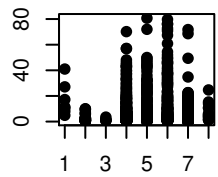
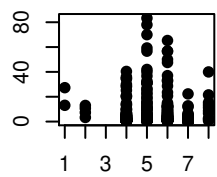
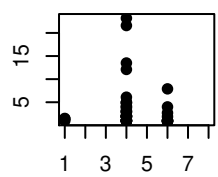
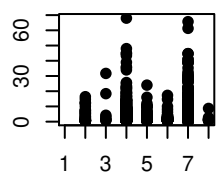
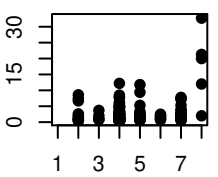
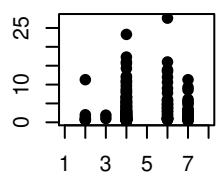
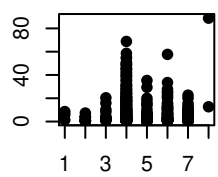
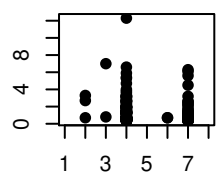
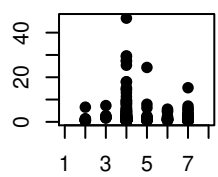
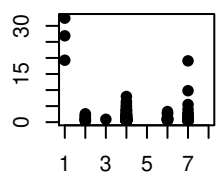
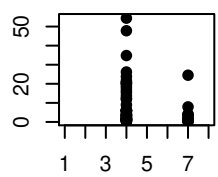
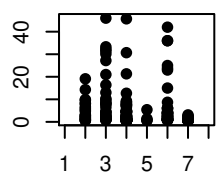
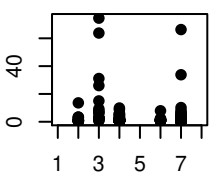
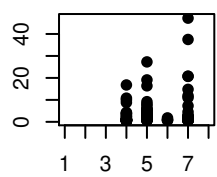
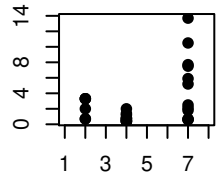
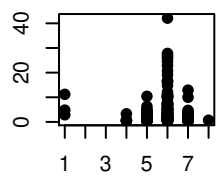
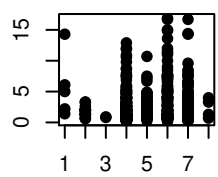
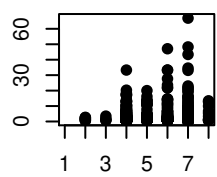
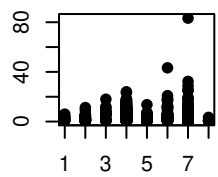
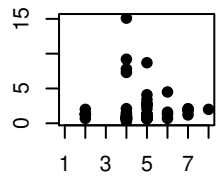
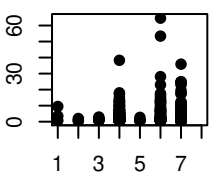
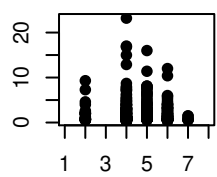
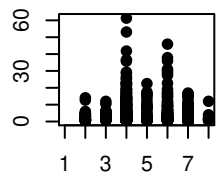
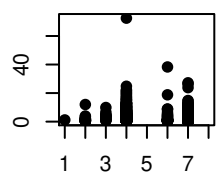
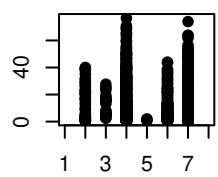
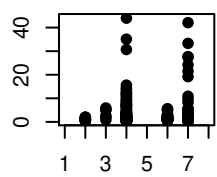
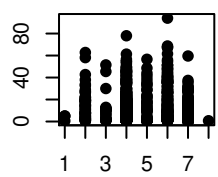
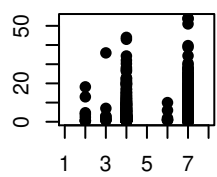
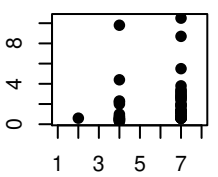
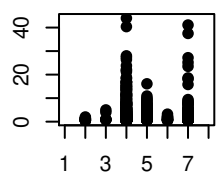
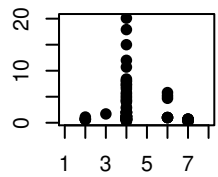
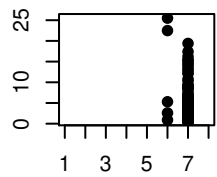
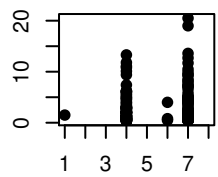
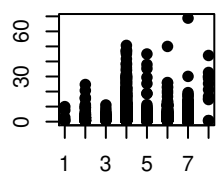
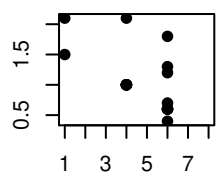
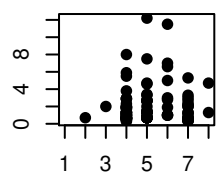
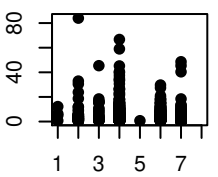
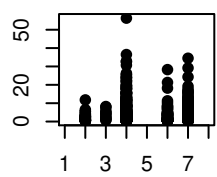
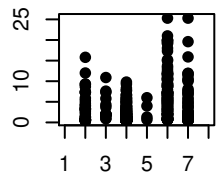
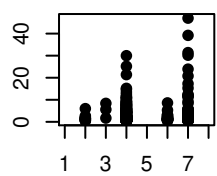
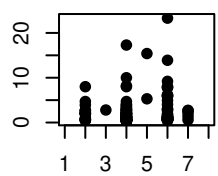
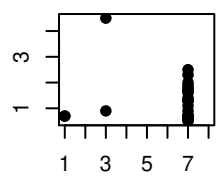
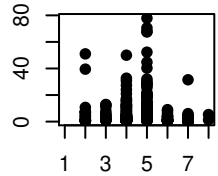
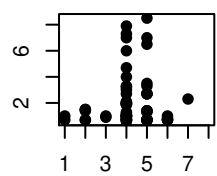
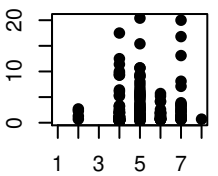
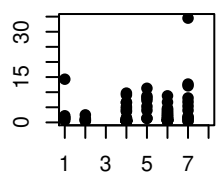
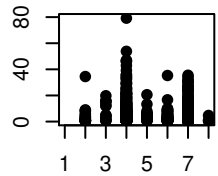
Figure S7: Comparison of water table depth optima (cm) for 64 taxa from the full dataset and five eco-region models (see text for details), ordered by the full dataset. Coloured spots represent optima of individual taxa in different models, grey bars represent range between the highest and lowest optima for each taxon. For references to colour, readers are referred to the online version of the article.

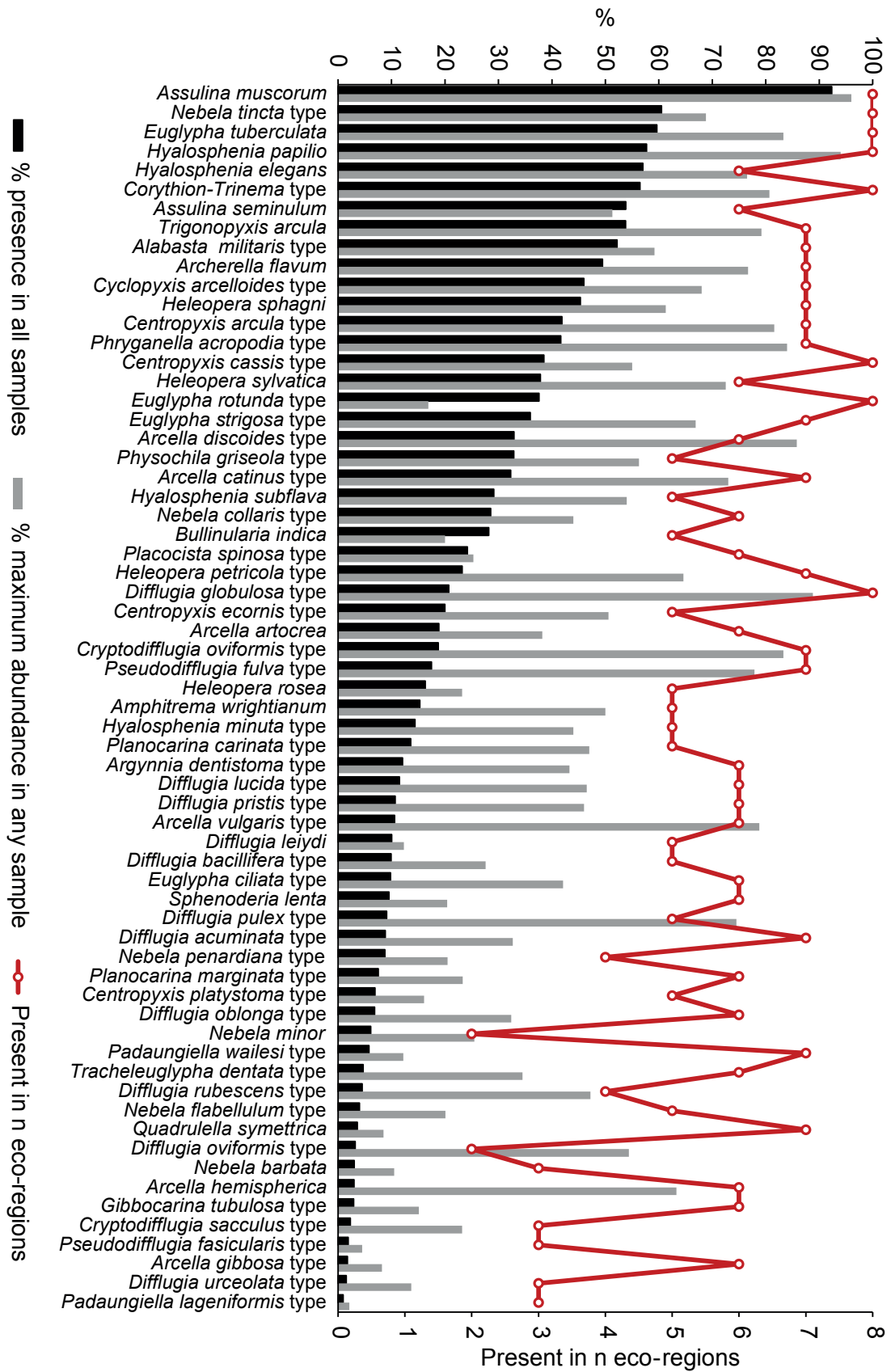








ALA MIL (983)**AMP WRI (288)****ARC ART (355)****ARC CAT (608)****ARC DIS (620)****ARC GIB (33)****ARC HEM (56)****ARC VUL (199)****ARC FLA (932)****ARG DEN (227)****ASS MUS (1740)****ASS SEM (1014)****BUL IND (531)****CEN ACU (789)****CEN CAS (725)****CEN ECO (376)****CEN PLA (130)****COR TRI (1064)****CRY OVI (353)****CRY SAC (43)****CYC ARC (866)****DIF ACU (166)****DIF BAC (187)****DIF GLO (390)****DIF LEI (189)****DIF LUC (216)****DIF OBL (129)****DIF OVI (60)****DIF PRI (201)****DIF PUL (171)****DIF RUB (85)****DIF URC (29)****EUG CIL (185)****EUG ROT (708)****EUG STR (677)****EUG TUB (1123)****GIB TUB (55)****HEL PET (437)****HEL ROS (307)****HEL SPH (854)****HEL SYL (713)****HYA ELE (1074)****HYA MIN (271)****HYA PAP (1087)****HYA SUB (549)****NEB BAR (57)****NEB COL (538)****NEB FLA (75)****NEB MIN (115)****NEB PEN (165)****NEB TIN (1140)****PAD LAG (18)****PAD WAI (109)****PHR ACR (785)****PHY GRI (619)****PLA SPI (456)****PLA CAR (256)****PLA MAR (142)****PSE FAS (36)****PSE FUL (329)****QUA SYM (68)****SPH LEN (179)****TRA DEN (88)****TRI ARC (1013)**



Modelled water-table depth optima (cm)

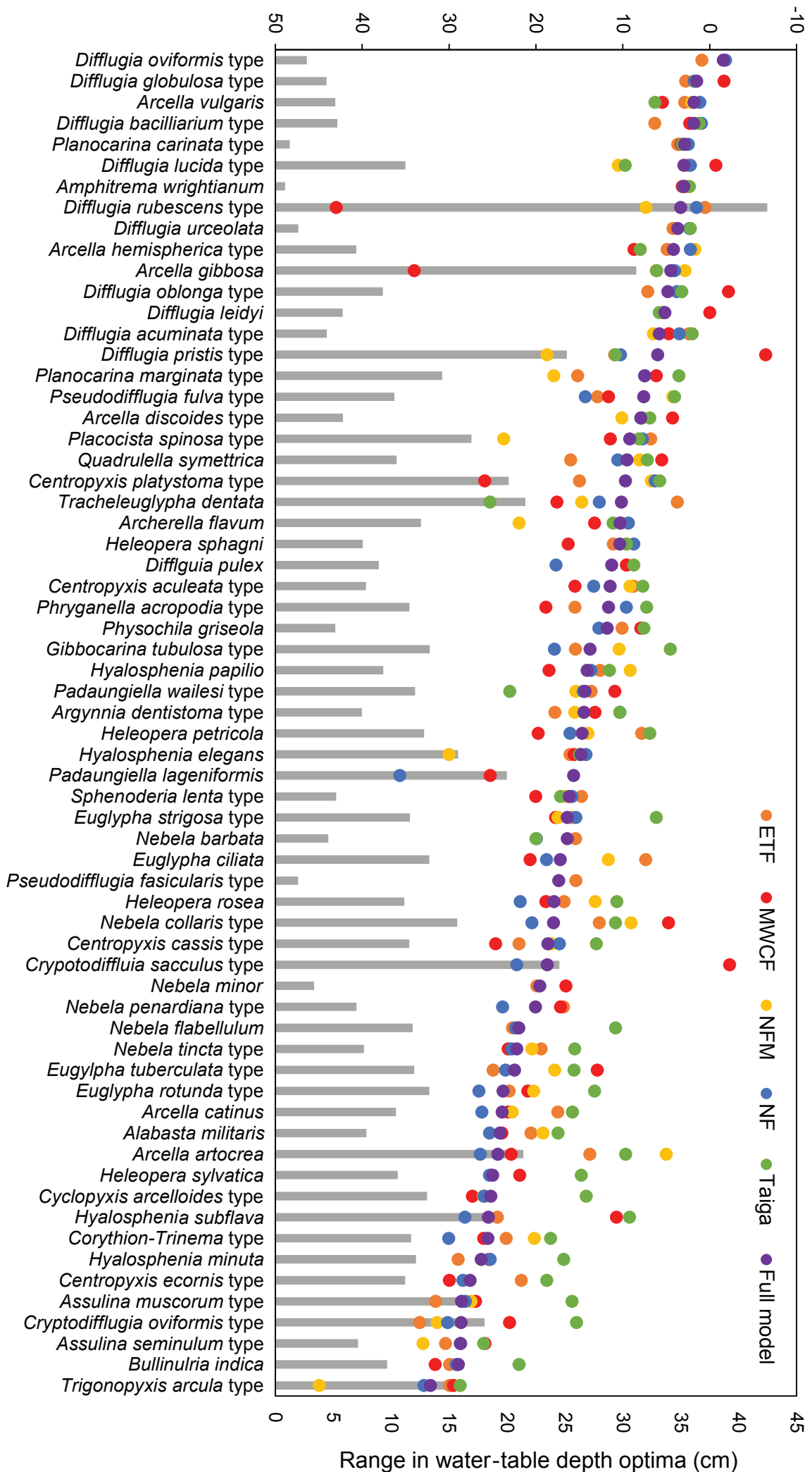


Table S1: Rare taxa removed from complete dataset, occurring in <1% of the total number of samples (i.e. <19).

Name	Abbreviation	Number of occurrences	Maximum abundance (%)
Coniocassis pontigulasiformis	CON PON	2	1.5
Cyphoderia ampulla	CYP AMP	8	1.9
Lesquereusia epistomum	LES EPI	1	0.5
Lesquereusia modesta type	LES MOD	6	12.4
Paraquadrula irregularis	PAR IRR	4	13.4
Plagiopyxis callida type	PLAGIO	2	1.1
Pyxidicula sp.	PYXI	9	10.1
Waileseila eboracensis	WAI EBO	2	0.8

Table S2: Samples removed where taxonomic merging or deletion of results only identified to species level resulted in a percentage total <90%.

Reference	Sample ID	Site	Remaining %
Finkelstein/Bunbury (unpublished)	M4	Attawapiskat River 1	89.1
Finkelstein/Bunbury (unpublished)	M17	Attawapiskat River 1	87.5
Finkelstein/Bunbury (unpublished)	M23	Attawapiskat River 1	85.6
Finkelstein/Bunbury (unpublished)	M24	Attawapiskat River 1	86.3
Finkelstein/Bunbury (unpublished)	M25	Attawapiskat River 1	79.8
Finkelstein/Bunbury (unpublished)	M28	Attawapiskat River 1	88.9
Finkelstein/Bunbury (unpublished)	M11	Attawapiskat River 2	89.0
Finkelstein/Bunbury (unpublished)	M42	Sutton River 2	88.2
Charman and Warner (1992)	1142	Wally Creek	89.2
Charman and Warner (1992)	1212	Wally Creek	88.4
Charman and Warner (1992)	12C12	Wally Creek	84.3

Table S3: Samples removed with extreme water-table depths (WTDs) (i.e. those below the 0.5th or above the 99.5th percentiles).

Reference	Sample ID	Site	WTD (cm)
Warner and Charman (1994)	NWO-BB	Unknown	82.0
Warner and Charman (1994)	NWO-N	Unknown	68.0
Warner and Charman (1994)	NWO-D	Unknown	100.0
Warner and Charman (1994)	NWO-E	Unknown	100.0
Warner and Charman (1994)	NWO-F	Unknown	100.0
Warner and Charman (1994)	NWO-G	Unknown	74.0
Roe et al. (2017)	MER17	Mer Bleue	82.0
Roe et al. (2017)	ALF18	Alfred	72.0
Sullivan and Booth (2011)	TA28	Tannersville	-16.5
Markel et al. (2010)	AK93	Brown's Lake	-17.0
Markel et al. (2010)	AK84	Brown's Lake	-16.5
Markel et al. (2010)	AK48	Gas field	-18.0
Booth (2002)	1020B	Au Train Bay	-27.0
Booth (2001)	967ada	Tahquamenon Bay	-21.0
Booth (2001)	968ada	Tahquamenon Bay	-26.0
Booth (2001)	832ada	Grand Traverse Bay	-21.0
Booth (2001)	832bda	Grand Traverse Bay	-37.0
Booth (2008)	AL06	Herron	75.0

Table S4: Rare taxa removed from the combined North American and European dataset, occurring in <1% of the total number of samples (i.e. <37).

Name	Abbreviation	Number of occurrences	Maximum abundance (%)
Arcella mitrata	ARC MIT	2	0.9
Campascus minutus	CAM MIN	11	19.7
Coniocassis pontigulasiformis	CON PON	2	1.5
Diffugia gramen type	DIF GRA	24	4.1
Lagenodiffugia vas	LAG VAS	8	3.7
Lesquereusia epistomum	LES EPI	15	3.3
Plagiopyxis type	PLAGIO	10	11.0
Pontigulasia elisa	PON ELI	1	0.7
Pseudodiffugia gracilis	PSE GRA	3	2.2
Pyxidicula type	PYXI	31	12.1
Waileseila eboracensis	WAI EBO	2	0.8

Table S5: Samples removed from the combined North American and European dataset where taxonomic merging resulted in a percentage total <90%.

Reference	Sample ID	Site	Remaining %
Bobrov et al. (1999)	KATIN_6	Katin Moch	53.4
Lamentowicz et al. (2013); Jassey et al. (2014)	WEK14	Wierzchołek	53.8
Lamentowicz et al. (2008)	CHL23	Chlebowo	59.1
Lamentowicz et al. (2013); Jassey et al. (2014)	WEK6	Wierzchołek	59.6
Lamentowicz et al. (2013); Jassey et al. (2014)	WEK11	Wierzchołek	59.8
Lamentowicz et al. (2008)	CHL22	Chlebowo	68.8
Finkelstein/Bunbury (unpublished)	M25	Attawapiskat River 1	69.7

Lamentowicz et al. (2013); Jassey et al. (2014)	WEK2	Wierzchołek	70.2
Lamentowicz et al. (2008)	CHL7	Chlebowo	72.6
Lamentowicz et al. (2013); Jassey et al. (2014)	RUR23	Rurzyca	75.6
Lamentowicz et al. (2010)	72	Lej Nair	75.8
Lamentowicz et al. (2010)	71	Lej Nair	78.1
Finkelstein/Bunbury (unpublished)	M23	Attawapiskat River 1	78.8
Lamentowicz et al. (2013); Jassey et al. (2014)	WEK13	Wierzchołek	79.0
Lamentowicz et al. (2013); Jassey et al. (2014)	WEK5	Wierzchołek	79.3
Finkelstein/Bunbury (unpublished)	M28	Attawapiskat River 1	79.6
Bobrov et al. (1999)	STAR_1	Staroselia	80.1
Lamentowicz et al. (2008)	CHL1	Chlebowo	80.4
Bobrov et al. (1999)	KATIN_7	Katin Moch	80.7
Finkelstein/Bunbury (unpublished)	M24	Attawapiskat River 1	81.2
Swindles et al. (2015)	C1	Crash	82.4
Charman and Warner (1992)	12C12	Wally Creek	84.3
Lamentowicz et al. (2013); Jassey et al. (2014)	WEK10	Wierzchołek	85.4
Turner et al. (2013)	TM85	Malham Tarn Moss	85.5
Mallon (unpublished)	GAL_3	Gallsereds mossen	85.7
Finkelstein/Bunbury (unpublished)	M44	Sutton River 2	87.0
Lamentowicz et al. (2013); Jassey et al. (2014)	WEK12	Wierzchołek	87.2
Finkelstein/Bunbury (unpublished)	M17	Attawapiskat River 1	87.5
Lamentowicz et al. (2013); Jassey et al. (2014)	KAZ3	Kazanie	87.9
Finkelstein/Bunbury (unpublished)	M42	Sutton River 2	88.2
Lamentowicz et al. (2013); Jassey et al. (2014)	RUR10	Rurzyca	88.4
Charman and Warner (1992)	1212	Wally Creek	88.4
Bobrov et al. (1999)	Q92_1	Tverskaya Reserve	88.6
Mallon (unpublished)	S11_8	South	89.0
Finkelstein/Bunbury (unpublished)	M11	Attawapiskat River 2	89.0
Swindles et al. (2009)	MO6	Moninea	89.0

Lamentowicz (unpublished)	K 09	Kuźnik	89.1
Finkelstein/Bunbury (unpublished)	M4	Attawapiskat River 1	89.1
Charman and Warner (1992)	1142	Wally Creek	89.2
Swindles et al. (2009)	MO32	Moninea	89.3
Lamentowicz et al. (2013); Jassey et al. (2014)	RUR15	Rurzyca	89.3
Lamentowicz et al. (2013); Jassey et al. (2014)	RUR22	Rurzyca	89.3
Lamentowicz (unpublished)	K 07	Kuźnik	89.7
Bobrov et al. (1999)	KATIN_5	Katin Moch	89.7
Swindles et al. (2009)	MO27	Moninea	89.9

Table S6: Samples removed from the combined North American and European dataset with extreme water-table depths (WTDs) (i.e. those below the 0.5th or above the 99.5th percentiles).

Reference	Sample ID	Site	WTD (cm)
Turner et al. (2013)	TM91	Malham Tarn Moss	-60
Turner et al. (2013)	TM61	Malham Tarn Moss	-50
Booth (2001)	832bda	Grand Traverse Bay	-37
Booth (2002)	1020B	Au Train Bay	-27
Booth (2001)	968ada	Tahquamenon Bay	-26
Lamentowicz (unpublished)	K 14	Kuźnik	-25
Booth (2001)	832ada	Grand Traverse Bay	-21
Booth (2001)	967ada	Tahquamenon Bay	-21
Lamentowicz et al. (2013); Jassey et al. (2014)	CZS14	Czarci Staw	-20
Lamentowicz et al. (2010)	30	Mauntschas	-20
Turner et al. (2013)	TM62	Malham Tarn Moss	-20
Markel et al. (2010)	AK48	Gas field	-18
Lamentowicz et al. (2013); Jassey et al. (2014)	WAG22	Wagowo	-17

Markel et al. (2010)	AK93	Brown's Lake	-17
Markel et al. (2010)	AK84	Brown's Lake	-16.5
Sullivan and Booth (2011)	TA28	Tannersville	-16.5
Turner et al. (2013)	TM69	Malham Tarn Moss	83
Lamentowicz (unpublished)	Sł26	Słowińskie Błoto	84
Lamentowicz (unpublished)	Sł27	Słowińskie Błoto	84
Lamentowicz (unpublished)	Sł28	Słowińskie Błoto	84
Lamentowicz (unpublished)	Sł29	Słowińskie Błoto	84
Turner et al. (2013)	ThM189	Thornton Moor	85
Mitchell et al. (1999)	S 22	Les Pontins	100
Mitchell et al. (1999)	S 23	Les Pontins	100
Mitchell et al. (1999)	S 44	Le Bois des Lattes	100
Warner and Charman (1994)	NWO-D	Unknown	100
Warner and Charman (1994)	NWO-E	Unknown	100
Warner and Charman (1994)	NWO-F	Unknown	100
Mitchell et al. (1999)	S 16	Le Cachot	120
Mitchell et al. (1999)	S 17	Le Cachot	120
Mitchell et al. (1999)	S 18	Le Cachot	120
Mitchell et al. (1999)	S 19	Le Cachot	120
Mitchell et al. (1999)	S 20	Le Cachot	120
Mitchell et al. (1999)	S 21	Le Cachot	150
Mitchell et al. (1999)	S 41	Le Bois des Lattes	150

Table S7: Summary of published peatland testate amoeba transfer functions in North America and Europe. $RMSEP_{LOO}$ and R^2 values are for the best performing model as selected by the authors of each publication (as shown in model type column). Data for number of sites and samples is for data-pruned version of model if this information is available, if not, then values are for the complete dataset. For model type: WA-Tol (inv) = weighted averaging with tolerance downweighting and inverse deshrinking; WA-Tol = weighted averaging with tolerance downweighting, no deshrinking method specified; WAPLS C2 = second component of weighted averaging partial least squares; WA = weighted-averaging, no deshrinking method specified, WA (inv) = weighted averaging with inverse deshrinking, ML = maximum likelihood.

Continent	Location	Number of sites	Number of samples	Model type	$RMSEP_{LOO}$ (cm)	R^2	Reference
North America	North America	126	1730	WA-Tol (inv)	7.42	0.72	This study
North America	Newfoundland	14	60	WA-Tol	6.32	0.71	Charman and Warner (1997)
North America	Michigan	2	74	WAPLS C2	7.48	0.61	Booth (2001)
North America	Michigan	11	139	WAPLS C2	7.51	0.74	Booth (2002)
North America	Alaska	8	101	WAPLS C2	9.7	Not given	Payne et al. (2006)
North America	Mid-continental and eastern USA	31	369	WAPLS C2	6.6	0.83	Booth (2008)
North America	North Carolina	1	33	WA	5.8	0.62	Booth et al. (2008)
North America	Alaska	12	126	WAPLS C2	4.6	0.86	Markel et al. (2010)
North America	Atlantic Canada and NE USA	18	225	WA-Tol (inv)	5.66	0.87	Amesbury et al. (2013)
North America	Québec	18	165	WA (inv)	5.44	0.8	Lamarre et al. (2013)
Europe	Europe	113	1302	WA-Tol (inv)	7.72	0.59	Amesbury et al. (2016)
Europe	Europe	8	119	WAPLS C2	5.6	0.71	Charman et al. (2007)
Europe	Great Britain	9	163	WA-Tol	3.93	Not given	Woodland et al. (1998)

Europe	Western Russia	6	31	WAPLS C2	5.16	0.83	Bobrov et al. (1999)
Europe	North-western Poland	3	45	WA-Tol	9.89	0.91	Lamentowicz and Mitchell (2005)
Europe	Greece	4	57	ML	2.48	0.68	Payne and Mitchell (2007)
Europe	Turkey	1	42	ML	7.1	0.81	Payne et al. (2008)
Europe	Western Poland	1	30	WA	6.99	0.4	Lamentowicz et al. (2008)
Europe	Northern Ireland	3	95	WA-Tol	4.99	0.83	Swindles et al. (2009)
Europe	England	6	116	WA-Tol (inv)	7.36	0.71	Turner et al. (2013)
Europe	Northern Sweden	9	59	WA-Tol (inv)	5.25	0.87	Swindles et al. (2015c)

MEAN:

6.33

0.74

STANDARD DEVIATION:

1.76

0.13